I give permission for public access to my thesis and for copying to be done at the direction of the archives' librarian and/or the College library.

_____ _____

Signature Date

A GENE EXPRESSION STUDY OF THE ALTERNATIVELY SPLICED b20 GENE IN THE FILARIAL PARASITE BRUGIA MALAYI

by

Rachael Bonawitz

A Paper Presented to the

Faculty of Mount Holyoke College in

Partial Fulfillment of the Requirements for

The Degree of Bachelors of Arts with

Honor

Department of Biological Sciences

South Hadley, MA 01075

May, 2005

This paper was prepared
under the direction of
Professor Craig Woodard
for eight credits.

ACKNOWLEDGMENTS

Firstly, my thanks to Professor Steven Williams for his willingness to take me in to the SAW Lab when I was worried about 'worm withdrawal.' Your enthusiasm and wealth of knowledge have been extremely helpful throughout this endeavor.

Thanks to all the members of the SAW Lab for the warm welcome and friendly advice, but especially Sue Haynes for your willingness to help in any capacity, Wen Li, for answering my many questions with infinite patience, and Lori Saunders for your RT-PCR expertise and saving me from the PVTA.

Most especially, I'd like to thank Sandra Laney for inspiring me with her total commitment to b20 and for helping me every step along the way. I am in awe of your dedication and determination. Without your encouragement, guidance, and attention to detail, this project would not have happened. Thank you for being such a patient teacher. I appreciate more than I am able to articulate the long hours you spent working with me despite the many demands on your time and energy. I have truly enjoyed working with you on what is, I'm now convinced, the most important filarial gene.

Thank you to Dr. Tom Nutman and everyone at the Helminth Immunology Section at the National Institutes of Health for the opportunity to work there for two fantastic summers, where I first met *Brugia malayi*. Special thanks, as always, to Dr. Kawsar Talaat, a mentor in every sense of the word.

Thanks to Professor Craig Woodard, who despite a hectic schedule, agreed to be my Mount Holyoke thesis advisor and always cheerfully made time to meet with me. Thank you to Professor Sharon Stranford, for your thought-provoking questions and consistent demand for the best work I am capable of producing. It is by your example and through your teaching that I have become a stronger thinker and scientist. Thank you to Professor Megan Nunez for enthusiastically agreeing to be my third reader.

Thank you to the entire Mount Holyoke College Department of Biological Sciences. A special thanks to my fellow Hughsies; without that wonderful summer (and three years since!) spent learning with you all, I don't know that I'd be where I am now. A heartfelt thank you to my parents for making my education at Mount Holyoke possible.

Last but not least, my thanks to my advisor, Professor Stan Rachootin. I know it seemed as though I rarely took your advice, but your unconditional support, willingness to listen, and eagerness to proof-read *everything* throughout the past three years has been invaluable to me. If life is a 'fluke,' I'm lucky to have had the opportunity to learn from you.

TABLE OF CONTENTS

LIST OF FIGURES

Page No.

LIST OF TABLES

ABSTRACT

Lymphatic filariasis, a disease caused by the parasitic nematode *Brugia malayi* and transmitted by mosquitoes, infects approximately 130 million people in eighty-three countries in the tropical/sub-tropical belt. *B. malayi* b20 (Bmb20), an ortholog of the nematode-specific gene *Onchocerca volvulus* b20 (Ovb20), has been identified as an alternatively-spliced gene, with at least four splice variants identified by plaque screenings of *B. malayi* cDNA libraries. The purpose of the following work is to evaluate the transcription patterns of Bmb20 splice variants in the various life cycle stages of the *B. malayi* parasite using both RT-PCR and quantitative RT-PCR methods. The evaluation of Bmb20 splice variants may result in the identification of a splice variant form specific to the third larval stage (L3) of *B. malayi*. This L3-specific form could be used as a target in a diagnostic assay to identify L3 infective mosquitoes and thus evaluate the transmission potential in endemic regions, a necessary component of the Global Programme to Eliminate Lymphatic Filariasis. Eight b20 splice variants were tested using RT-PCR and none appeared to be L3-specific, though two forms did appear to be upregulated in the L3 stage. Quantitative RT-PCR experiments with one of these forms, b20-l, indicates that with respect to most life cycle stages, the b20-l variant is upregulated in L3. However, further studies are necessary in order to assess the level of expression in comparison to other larval stages. This study illustrated that RT-PCR and qRT-PCR are useful methods in the detection of gene expression.

INTRODUCTION

Lymphatic filariasis

Lymphatic filariasis is a disease caused by the parasitic nematodes *Wucheria bancrofti*, *Brugia malayi*, and *Brugia timori*. Lymphatic filariasis, while rarely fatal, accounts for nearly five million diasbility adjusted life years and is a major cause of clinical suffering in tropical and subtropical areas of the world (World Health Organization, 2001). Lymphatic filariasis is endemic in eighty-three countries in the tropical/sub-tropical belt, and more than one billion people live at risk of infection in these areas (Figure 1) (Cox, 2000). Approximately 130 million people have lymphatic filariasis. Most infections are acquired during childhood and later progress to the clinical pathologies associated with chronic disease, such as elephantiasis (grossly swollen limbs) and hydrocele (fluid-filled scrotum) (WHO, 2001). It is estimated that of those 130 million people infected with lymphatic filariasis, 25 million men suffer from hydrocele, and 15 million people have lymphedema or elephantiasis, most commonly of the lower extremities. Among parasitic diseases, only malaria, which kills more than one million people a year, ranks as more debilitating (WHO, 2001; WHO, 2000).

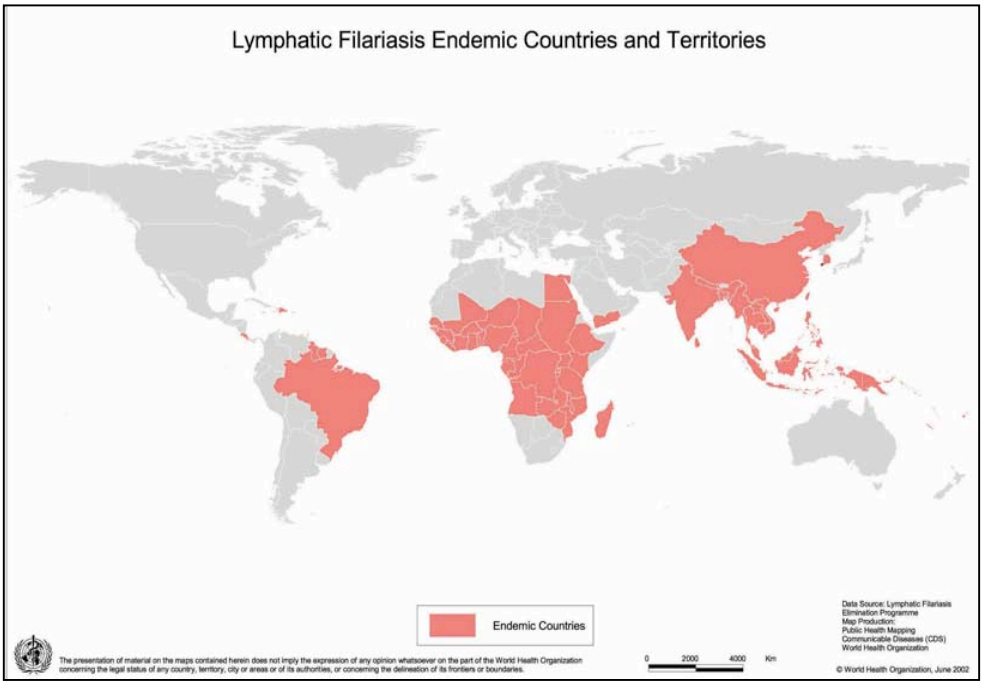

Figure 1. Geographic map of the tropical and subtropical regions of the world endemic for lymphatic filariasis (both Brugian and Bancroftian). Approximately eighty-three countries are included in this geographic range. More than 150 million individuals are currently infected, with more than one billion at risk. (Image available at http://www.filariasis.org/index.pl?id=2923)

Brugia malayi

Of the three causative agents of lymphatic filariasis, *B. malayi*, restricted in geographic range to Asia, is responsible for nine percent of infections. *W. bancrofti*, found in all endemic areas, causes ninety-one percent of all infections (Scott, in *Lymphatic Filariasis*, 2000). *B. timori*, also restricted to Asia, is responsible for only a small fraction of infections worldwide (WHO, 2001). There is a close phylogenetic relationship between *W. bancrofti* and *B. malayi,* both of the family Onchocercidae (Xie *et al*, 1994). A lack of clearly homologous characters has prevented the derivation of a consistent evolutionary framework for the phylum Nematoda (Blaxter *et al.*, 1998).

Although *W. bancrofti* is responsible for the majority of infections, it is an obligate human parasite with a life cycle that cannot be maintained in an animal model. The *B. malayi* lifecycle can be maintained in gerbils, which are considered to be a good animal model, because *B. malayi* causes the same disease in gerbils as in humans. Therefore, *B. malayi* is more often used for research purposes in the laboratory because of the readily available parasite material.

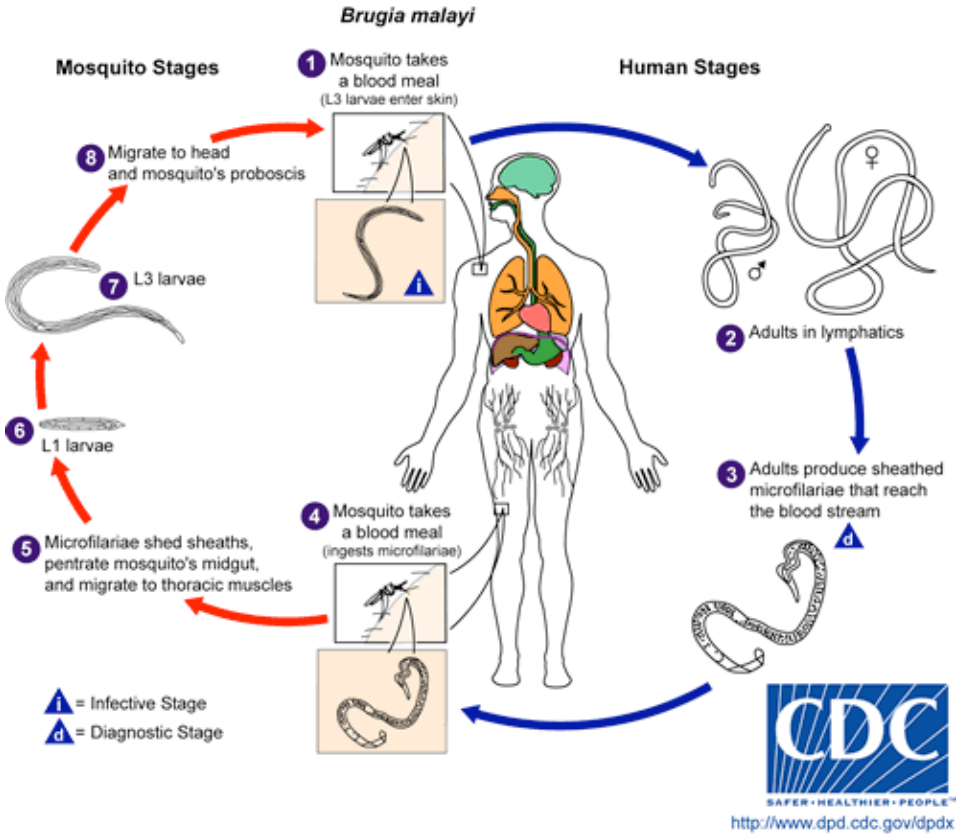

Figure 2. Diagram of the life cycle of *Brugia malayi*, shown alternating between the human host and mosquito vector. During a blood meal, an infected mosquito introduces third-stage filarial larvae onto the skin of the human host, where they penetrate into the bite wound (1) and then migrate to the lymphatics (2). Female worms produce millions of microfilariae, which circulate in the blood until being ingested by a mosquito taking a blood meal (4). After ingestion, the microfilariae develop to the L3 stage in the mosquito gut before migrating to the prosbocis, primed to infect another human when the mosquito takes a blood meal. (Image available at http://www.dpd.cdc.gov/dpdx/HTML/Filariasis.asp?body=Frames/AF/Filariasis/body_Filariasis_b_malayi.htm).

Life Cycle of Brugia malayi

The three species of lymphatic dwelling filariae have a complex life cycle that alternates between the mosquito vector and the human host (Figure 2). Transmission is exclusively via mosquito vectors, though the competent species of mosquito varies with geographic location. Mosquitoes transmit the third larval (L3) stage of the parasite to humans when taking a bloodmeal (puncturing human flesh). Upon entry into the human host, the L3 larvae migrate to the nearest afferent lymphatics, molt to the fourth larval (L4) stage and undergo a final molt into sexually mature adults. After sexual reproduction, adult females produce millions of sheathed microfilariae (mf) that migrate to and circulate in the bloodstream, usually in synchrony with diurnal mosquito feeding patterns (Scott, in *Lymphatic Filariasis*, 2000; Keiser and Nutman, 2002). During subsequent bloodmeals, these mf are then picked up by mosquitoes. In the abdomen of the mosquito, the mf mature to the first larval stage (L1), and undergo two molts, becoming second larval stage (L2), and then human infective L3 larvae (Scott in *Lymphatic Filariasis*, 2000; Bain and Babayan, 2003).

From beginning to end, the duration of the *B. malayi* lifecycle is as follows: in the mosquito gut, the molt from L1 to L2 ranges from six to ten days, and the molt from L2 to L3 takes one to three days. Thus, it takes approximately two weeks for the infective L3 larvae to mature in the vector. Following a bite from an infective mosquito, and the entry of L3s into human

skin, the molt from L3 to L4 ranges from nine to fourteen days in the human host, as the worm is migrating through the circulatory system to the lymphatics. The final molt, from the L4 stage to the adult worm, requires a minimum of three months, but may last as long as twelve months, and is localized in the lumen of dilated lymphatic vessels, the final site of the adult worm in the human body (Bain and Babayan, 2003). While the precise length of time has not been determined, adult worms remain reproductively active (continuously producing mf) for at least five years (Keiser and Nutman, 2002).

Pathology and Immunology of Lymphatic Filariasis

Chronic infection with filarial nematodes results in a wide spectrum of clinical pathologies, though patients have traditionally been classified as being at one immunological extreme or the other. At one extreme are infected individuals with detectable circulating microfilariae (microfilaremia) but without any detectable signs of pathology. These individuals, identified as asymptomatic microfilaremics, are assumed to be immunologically hyporesponsive to the parasite and unlikely to progress to clinical pathology (Freedman, 1998). At the other extreme are infected individuals with clinical evidence of lymphatic obstruction (such as elephantiasis), classified as having clinical filariasis. These individuals are typically amicrofilaremic and are generally assumed to have relatively strong immune responses to the parasite (Freedman, 1998). Despite the persistence of the concept of immune

polarization in LF and disease progression, the results of a long-term study conducted over a thirty-seven year period showed that microfilaremic and amicrofilaremic individuals are equally likely to have chronic pathological manifestations of disease (Michael *et al.*, 1994). While clinically asymptomatic individuals with microfilaremia *always* have active infection, it is more difficult to determine whether amicrofilaremic individuals with clinical filariasis are also actively infected with living adult worms. A better measure of infection status in clinical lymphatic filariasis may be the presence or absence of circulating filarial antigen, rather than circulating mf. Freedman (1998) suggests that the presence or absence of antigenemia, rather than overt clinical manifestations of the disease, is closely associated with specific immunological and cytokine responses (Freedman, 1998).

Amicrofilaremic individuals with clinical filariasis have previously been shown to have relatively increased *in vitro* immunological reactivity to filarial antigen, while asymptomatic microfilaremics have been shown to have relative cellular immunological hyporesponsiveness to filarial antigen *in vitro* (Baird *et al*, 2002). Asymptomatic microfilaremic individuals produced and secreted less IFN-γ, a Th-1 type cytokine, in response to antigenic stimulation than individuals with clinical filariasis (deAlmeida *et al.*, 1998). Thus, individuals who are actively infected (microfilaremic) yet asymptomatic (no signs of clinical pathology) demonstrate a decreased inflammatory response to the parasite compared to those individuals with chronic pathologies. Recent

studies have shown that upon antigenic stimulation, IL-4 production and secretion were not significantly different in asymptomatic individuals and individuals with clinical filariasis (deAlmeida *et al.*, 1998). IL-4 is a Th-2 type cytokine, and indicates an immune response dependent on antibody production, typically parasite-specific IgE and IgG4 in the case of lymphatic filariasis (Hussain *et al*., 1981; Ottesen *et al.*, 1985). Therefore, infection status (antigenemia vs. no antigenemia) rather than clinical status (clinical manifestations versus none) appears to be closely associated with the segregation of cytokine response patterns. However, studies conducted after treatment of both Brugian and Bancroftian filariasis with the antifilarial drugs diethylcarbamazine (DEC) and ivermectin have determined that the clearance of circulating filarial antigen to undetectable levels may take as long as six months after the presumed clearance of adult worms (Eberhard *et al*., 1997; Weil *et al*., 1998).

The most common clinical manifestations of chronic disease are lymphedema and elephantiasis of the extremities, as well as of the genitals, particularly hydrocele in males (Figure 3). Adenolymphanganitis (ADL) is an additional acute manifestation of clinical filariasis and encompasses several episodes a year of acute inflammatory disease, such as fevers and localized, painful lymphatic swelling, associated with the death of adult worms, as well as opportunistic infections by bacteria and fungi (as described by Taylor, 2002; Nutman and Keiser, 2002). The manifestations of chronic pathology are in

part caused by the lymphatic vessel destruction and obstruction of lymph due to the presence of adult worms in the lumen of lymphatic vessels (Kumarasawmi in *Lymphatic Filariasis*, 2000). While inflammatory damage may be caused by the local immune response to parasite antigen, mechanical damage to the lymph vessels due to the whip-like action of the constantly motile adult worms, as well as the possible toxic effects of parasite excretory-secretory products, also contribute to the degree of disease and damage in LF (Freedman, 1998). Additionally, pathology may be associated with the host immune response to dead and dying worms in the body (Dreyer *et al*, 2000).

B. malayi has an intracellular bacterial endosymbiont, *Wolbachia* (O'Neill *et al*., 1992). *Wolbachia* belong to a group of rickettsia-like obligate bacteria infecting a wide range of arthropods and nematodes; the generic term *Wolbachia* is used to indicate the phylogenetic group that encompasses the closely related arthropod *Wolbachia* and the filarial *Wolbachia* (Bandi *et al.*, 1998). In filarial worms such as *B. malayi*, *Wolbachia* are distributed throughout the hypodermis and female reproductive organs and facilitate filarial reproduction; loss of *Wolbachia* results in decreased micofilaria reproduction (Keiser and Nutman, 2002; Townson *et al*., 2000). Living filarial parasites seem to induce little inflammation themselves, but can cause acute inflammatory reactions when they die. The release of *Wolbachia* from the

a.

b.

Figure 3 a. An individual with gross elephantiasis of the right leg, and lymphedema of the left. While this person may not be actively infected (harboring live worms), at this point of disease progression, the damage is irreversible. Such lymphatic obstruction and damage can result in opportunistic fungal and bacterial infections of the affected extremity. Chronic pathologies of lymphatic filariasis contribute not only to a very poor quality of life in addition to decreased economic productivity, but also significant social stigmatization. 4b. Hydrocele, a common manifestation of bancroftian filariasis, affects approximately 15 million men worldwide. Less common but still prevalent in lymphatic filariasis disease is the occurrence of both breast and genital elephantiasis in women. (Images available at www.filariasis.org and faculty.gvsu.edu/ grahamdo/LFphotos.htm).

dead and dying worms, and thus the release of bacterial endotoxin and/or lipopolysaccharide, may be the cause of this acute inflammation (Taylor, 2002).

Global Programme to Eliminate Lymphatic Filariasis

Filarial infections are a significant cause of disability in the tropical areas of the world, and the chronic pathologies of lymphatic filariasis are physically debilitating, economically costly, and socially stigmatizing (Evans *et al*., 1993). Once the disease has progressed to the elephantiasis stage, it is irreversible (even if there is no active infection) but the infection burden in endemic communities can be reduced with the effective chemotherapeutic agents ivermectin, albendazole, and diethylcarbamazine (DEC) (reviewed in Keiser and Nutman, 2002). Two drug combinations, most commonly DEC and albendazole, effectively kill the circulating microfilariae and greatly reduce the fecundity of adult worms (Molyneux and Zagaria, 2002). This in turn reduces the uptake of microfilariae by the mosquito vector, and thereby disrupts transmission in endemic communities. Due to the development of these effective treatments within the last two decades, in addition to improved diagnostic methods for monitoring infection rates, global eradication of lymphatic filariasis began to be seriously considered as a feasible public health venture by the WHO (Ottesen, 2000).

The Global Programme to Eliminate Lymphatic Filariasis, initiated in May 1997, consists of two main goals: to interrupt the transmission of infection, and to alleviate and prevent the suffering and disability caused by the disease (Molyneux and Zagaria, 2002; Ottesen, 2000). Implementation of the GPELF began in 2000 with mass drug administration in a select twenty-two endemic countries, with the goal of global elimination of LF by the year 2020 (Molyneux and Zagaria, 2002). By the year 2001, 25.89 million people in 22 countries had been treated, a significant increase compared to the 2.9 million in 12 countries annually treated prior to the year 2000 (Molyneux and Zagaria, 2002).

Successful implementation of a similar drug administration campaign using ivermectin had proven effective in controlling onchocerciasis, commonly known as river blindness, in some regions of West Africa (Molyneux and Davies, 1997). Onchocerciasis, caused by the closely-related filarial parasite, *Onchocerca volvulus*, is a disease associated with dermal lesions resulting in both severe itching and depigmentation, and ocular lesions resulting in blindness (Abdel-Wahab *et al*.,1996). Both dermal and ocular lesions are caused by the host inflammatory response to dead and dying *O. volvulus* microfilarae (Despommier *et al.*, 1995). The life cycle of *O. volvulus* is very similar to *B. malayi*, except it is transmitted by *Simulium* species (black flies), instead of mosquitoes.

The Filarial Genome Project and Brugian Genomics

To aid in the elimination of filarial diseases, much research has focused on finding vaccine candidates and drug targets using molecular and immunological tools. Both *B. malayi* and *O. volvulus* genome projects were undertaken in the Williams' laboratory at Smith College to identify genes being expressed in the different life cycle stages of the parasites (Williams and Johnston, 1999; Williams *et al*., 2002a). The original objectives of the FGP were: 1) the identification of novel genes from cDNA libraries derived from all life cycle stages of *B. malayi*; 2) the construction of genomic libraries and the subsequent mapping of the *Brugia* genome; 3) the implementation of globally accessible databases and resources for analysis; and 4) the dissemination of filarial genome data and materials (Ghedin *et al.*, 2004, Williams and Johnston, 1999).

Prior to the initiation of the FGP, very few *Brugia* genes had been cloned. Because of the large genome size of the organism, estimated to be between 85 to 95 megabases, it was determined that the first priority for the project would be gene discovery (Williams and Johnston, 1999). To increase the catalogue of known genes, the genes were to be identified by the expressed sequence tag (EST) approach (Williams and Johnston, 1999). EST analysis is particularly useful in determining the relative level of gene expression in

different developmental stages, estimated by the relative abundance of that gene's cognate ESTs sequenced from the cDNA libraries of different stages. To test specificity, gene-specific primers were designed for the gene of interest and then used in PCR reactions to test all of the cDNA libraries. If the PCR indicated that cDNA clones for that gene were found in only one stage of development, then the gene was classified as being putatively stage-specific (Blaxter *et al.,* 1996; Blaxter *et al*., 1999; Williams and Johnston, 1999). The caveat of EST analysis is that each gene is represented in a cDNA library at approximately the same abundance as its mRNA. Thus, the cDNAs from constitutively expressed genes, such as house-keeping enzymes or cytoskeletal proteins, will be selected and sequenced repeatedly, while rare transcripts, such as transcription factors, will be selected rarely, if at all. As an EST project progresses, the probability of identifying new genes drops as the sequence set grows (Blaxter *et al.*, 1999).

18,741 ESTs derived from the cDNA libraries have been sequenced as of April 2005 (Nembase). The ESTs have been clustered into about 8,392 unique genes using TIGR and NEMBASE algorithms (Nembase, Ghedin *et al.*, 2004). The discovered genes have been classified via BLASTX analysis, with about eighty percent being nematode specific, and about thirty-eight to forty percent of those being filarial specific (Blaxter *et al.*, 1999; Williams and Johnston, 1999). While some genes appear to be stage-specific, the functions of many of these genes are unknown because very few have database

homologues and are probably unique to filarial species (Williams and Johnston, 1999; Ghedin *et al.*, 2004).

In April 2004, the genome of *B. malayi* was the first parasitic nematode genome to be sequenced, following the sequencing of the genomes of the non-parasitic nematode *C. elegans* in 1998 (Ghedin *et al.,* 2004, The *C. elegans* Sequencing Consortium, 1998). *B. malayi* contains two additional genomes besides the nuclear genome; the14 kb circular mitochondrial genome and the circular genome of the endosymbiotic bacterium *Wolbachia* (Bandi *et al.,* 1998; Foster *et al*., 2005). The sequencing of the *B. malayi* genome, as of April 2004, was ongoing. At least 75 Mb of the genome sequence has been assembled into scaffolds, which are comprised of oriented and ordered fragments interspersed with gaps. These scaffolds and other long contiguous fragments currently available were used in preliminary analysis of the genome (Ghedin *et al.*, 2004). The primary comparator for the *Brugia* genome is *C. elegans*, for which the complete genomic sequence is available (Blaxter *et al.*, 1999). Though in the phylum Nematoda, the position of *C. elegans* with respect to filarial parasites is not clear (*B. malayi* and *C. elegans* are estimated to have last shared a common ancestor about three hundred to five hundred million years ago), *C. elegans* remains the most reasonable standard to compare to *B. malayi* (Burglin *et al.*, 1998; Guilano *et al.*, 2002).

Though the sequencing of the genome has been significant, functional analysis is the next important step, as the functions of most of the tagged genes

are unknown (Foster and Johnston, 2002). While knowing the expression profile of a gene is important, gene regulation is also important, particularly in understanding and interrupting the life-cycle of disease-causing parasites. New technologies available for use include cDNA microarrays, which enable a shift from examining individual genes to looking at overall patterns of gene expression and the elucidation of comprehensive functional networks (Martin and Pardee, 2000).

Ovb20

OvB20 (capitalization referring to the protein; the gene is referred to as Ovb20) is an antigen of *O. volvulus* that was identified by immunoscreening using sera from cattle immunized with irradiated *O. lienalis* L3 larvae, a closely related cattle parasite (Abdel-Wahab *et al.*, 1996). Ovb20 is a single copy gene that is believed to be nematode-specific (Taylor *et al*., 1995; Abdel-Wahab *et al*., 1996). *In situ* hybridization experiments showed the transcription of Ovb20 to be predominantly confined to the larval stages of *O. volvulus*, with initiation in embryos and maximum production during the L3 to L4 molt (Abdel-Wahab *et al.*, 1996). However, some transcripts have been identified by PCR in both the adult male and adult female *O. volvulus* cDNA libraries, suggesting that there may be some level of transcription in adult worms. It is possible that the transcripts found in the adult females may be due to developing embryos in utero (Laney, personal communication). While the

functions of Ovb20 are currently unknown, its high level of expression during the L3 to L4 molt may indicate its importance at that time or its possible role in regulating some aspect of development.

Orthologs of Ovb20 have been found in other parasitic nematodes such as *Acanthocheilonema viteae*, *B. malayi*, *O. ochengi*, and *W. bancrofti* (Abdel-Wahab *et al.*, 1996). *C. elegans*, a free-living nematode, has an ortholog of b20 called gut exterior interacting protein 16 (gei-16). In *C. elegans*, gei-16 is required for ventral enclosure and elongation during embryonic development, larval development, and normal rates of postembryonic growth (Fraser *et al.*, 2000). RNAi knockouts of gei-16 resulted in lethal larval phenotypes, indicating its essential role in development in *C. elegans* (Fisk Green *et al.*, 2004). Therefore, Ovb20 might play a similarly essential role in development in filarial nematodes.

Studies using OvB20 in a vaccination trial in the rodent model of onchocerciasis identified it as a promising vaccine candidate (Taylor *et al.*, 1995). While the rodent model is not a fully permissive animal model of onchocerciasis, it does mimic the invasion and establishment of microfilariae in human skin. Recombinant B20 was injected into mice and gerbils that were subsequently challenged with infective *O. volvulus* L3 larvae. Immunization with the recombinant B20 did not induce a reduction in the number of mf recovered in the mice 2 weeks post-infection with *O. volvulus* L3s, but did induce a 49 to 60% reduction in adult worm recoveries, thus showing

protective capabilities of b20 (Taylor *et al*., 1995). The localization of b20 in the worm hypodermis and cuticle, plus its increased level of expression in the infective stage, also contributes to its promise as a vaccine candidate (Taylor *et al*., 1995).

B20 was thus one of eight vaccine candidates chosen for further field vaccine trials in an *O. ochengi* bovine model of onchocerciasis (Laney, 2002). It was during the cloning of the *O. ochengi* b20 ortholog for this multiunit field vaccine trial that the first b20 splice variant was identified (Laney, 2002). Comparison of the *O. ochengi* sequence with the *O. volvulus* sequence showed a 99.4% identity at the nucleotide level except for a 405 bp region that was missing from the *O. ochengi* clone. It was unknown whether this difference was due to a species difference, or due to the process of alternative splicing, wherein multiple transcripts known as splice variants can be generated from a single gene via post-transcriptional processing of precursor mRNA (pre-mRNA). The finding of a b20 splice variant in *O. ochengi* led to the plaque screenings of the available *O. ochengi* and *O. volvulus* cDNA libraries using a T3 forward vector primer and a specific b20 reverse primer (Laney, 2002). A total of three splice variants were found in *O. ochengi*, and thirteen Ovb20 splice variants were found across the different developmental stages of *O. volvulus:* mf, L2, L3, L3M (L3 molting stage), AF and AM (Laney, 2002).

Plaque screening experiments of the OvL3 and 3M cDNA libraries identified thirteen different b20 splice variants in *O. volvulus,* with several of

these b20 splice variants apparently expressed in a stage-specific manner (Laney, 2002). Five splice variants were found to be putatively expressed in the *O. volvulus* L3 stage, with only two of the *O. volvulus* splice variant forms found in more than one stage (Figure 4). Subsequent PCR amplification of OvL3 cDNA libraries verified the expression pattern identified in the plaque screens. Though Ovb20 was the first demonstrated case of alternative *cis*-splicing of a gene in a human filarial parasite, the complete genomic sequence of Ovb20 remains unknown because these plaque screening experiments were performed on amplified cDNA libraries and not at the RNA level.

Previous work with Bmb20, the *B. malayi* b20 ortholog, has identified a number of splice variants in this parasite. Four splice variants were previously identified in a plaque screening of a *B. malayi* L3 cDNA library and these Bmb20 splice variants were found only in the L3 stage (Walls, 2001). These four splice variants corresponded to four of the b20 forms also found in a simultaneous screening of the *O. volvulus* cDNA library. A full expression profile of the splice variants in *B. malayi* has yet to be determined. Additionally, though the genome of *B. malayi* has been sequenced, there is a lack of genomic information concerning one upstream region of b20, where the exons 50-22-24, believed to be constitutively expressed, are located (Figure 5).

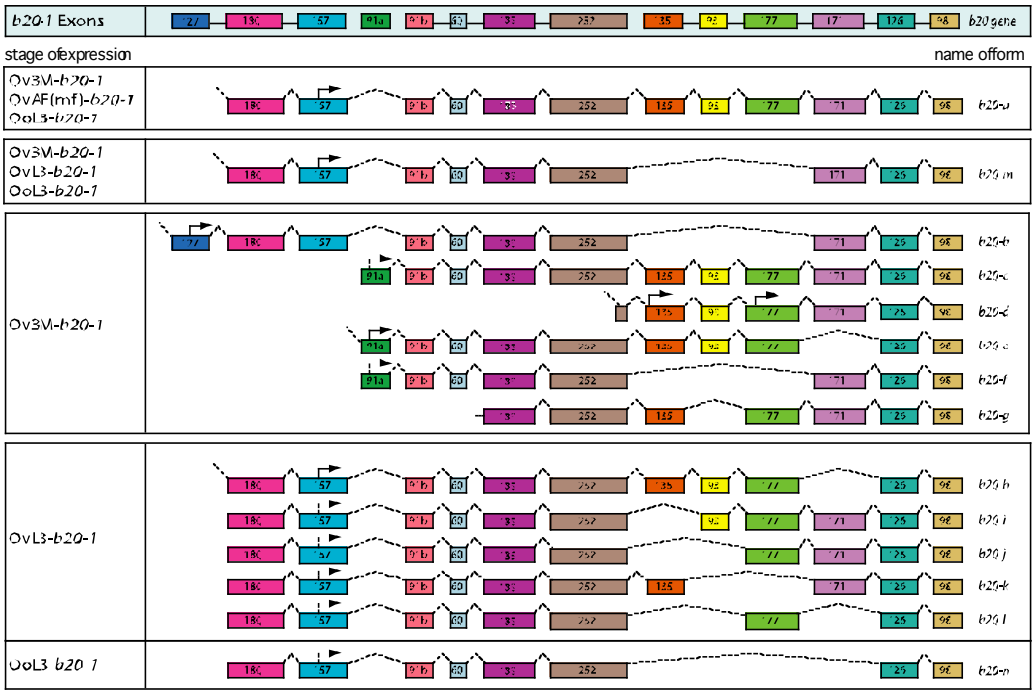

Figure 4. Exon pattern of b20 splice variants previously identified in *O. volvulus* and *O. ochengi*. The top box contains all of the known exons of the b20 gene in *O. volvulus*. Each form is represented showing the exons contained (exons represented by shaded boxes) and grouped according to which life cycle stage it was found to be expressed in. (Reprinted with permission of Sandra Laney).

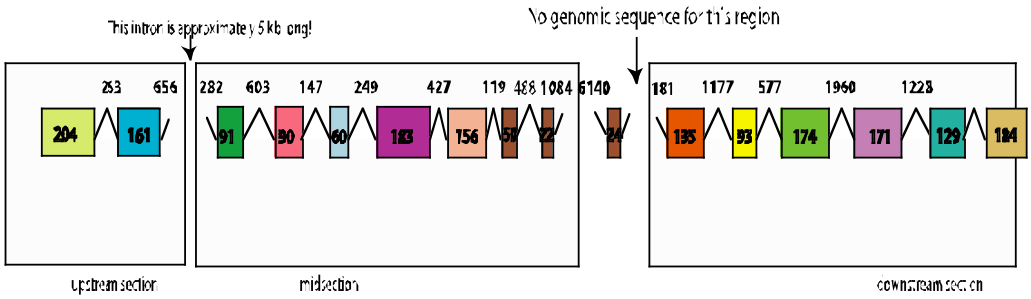

Figure 5. Known exons and introns of the b20 gene in *B. malayi*. Intron regions as verified by genomic sequence data are represented by the black numbers (indicating the size of the intron in bp) spanning exon regions. Exons are represented by shaded boxes with the size of the exon (in bp) included inside. Note the absence of sequence data concerning the region immediately downstream of exon 24.

Alternative Splicing and Ovb20

Alternative splicing is a mechanism used to expand the proteome of an organism. It is a process wherein more than one transcript can be generated from a single gene via post-transcriptional processing of precursor mRNA (pre-mRNA) (Gravely, 2001). These multiple transcripts encode different proteins, presumably with different functions, that may have significant biological consequences in an organism (Brudno *et al.*, 2001). While DNA recombination and the poorly-understood process of RNA editing are also processes that increase the number of proteins that can be synthesized from each gene, alternative splicing is the mechanism most widely used to expand protein diversity without expanding the genome (Gravely, 2001). To date, alternative splicing has been characterized in organisms ranging from yeast to humans, with as many as thirty percent of human genes estimated to be alternatively spliced, and about seventy percent of the pre-mRNAs in *C. elegans* estimated to be alternatively spliced (Brudno *et al.*, 2001; Blumenthal and Steward, 1997).

In parasitic nematodes, alternative splicing has been identified as the mechanism responsible for the sex-specific transcript of furin, an extracellular convertase, in *Dirofilaria immitis*, a filarial parasite of dogs and cats worldwide (commonly known as heartworm) (Jin *et al.*, 1999). Alternative splicing of a serotonin receptor has also been identified in the pig intestinal

parasite *Ascaris suum* (Huang *et al.*, 1999). Increasing evidence for other alternative splicing mechanisms has been found with the filarial nematodes *A. viteae* and *B. pahangi*. The excretory-secretory product, ES-62, important in mediating the host immune response to these worms is stage-specific with regard to protein production, though not with regard to constitutive mRNA production. A possible explanation for the constitutively expressed ES-62 mRNA, but the presence or absence of protein with respect to life-cycle stage, may be another example of alternative splicing in filarial nematodes (Stepek *et al.*, 2004).

While it has been hypothesized by Gravely (2001) that alternative splicing events may be the result of 'noise' (a mistake made by splicing machinery or an alternative exon without any function), the identification of thirteen b20 splice variants in *O. volvulus* and at least five splice variant forms in *B. malayi*, different species than *O. volvulus*, suggests that the alternative splicing of b20 in both organisims is not the result of 'noise'. Alternative splicing of gei-16, the C. elegans b20 ortholog, further supports the hypothesis that this phenomena is not the result of noise. The complex alternative splicing pattern of b20 in at least two filarial parasites*, O. volvulus* and *B. malayi* suggests an important and essential role for the b20 gene in these parasites, perhaps connected to having to adapt to a range of hosts throughout their lifecycles.

Purpose of the project

I am evaluating the transcription patterns of b20 splice variants in all of the life cycle stages of *B. malayi* using both RT-PCR and quantitative RT-PCR methods. Most genes in these parasites have been identified via EST analysis, and because ESTs do not include the entire coding regions of all genes, many different splice variants may go undetected in the database. Additionally, because alternative splicing may be restricted to specific tissues or stages of development, the different alternatively spliced forms of Bmb20 may not be well-represented in existing EST databases. RT-PCR is an alternative method for studying gene expression at the RNA level, and quantitative RT-PCR can be used to further compare and quantitate expression of selected genes.

There are several reasons to examine the expression pattern of the b20 splice variants, not the least of which is to attempt to identify either an L3-specific transcript, or a transcript present in no larval stages other than L3. An infective-stage b20 splice variant could be used in a diagnostic assay for infect*ive* (as opposed to infect*ed*) mosquitoes in endemic areas, for which an RT- PCR assay is currently being developed. Infect*ive* mosquitoes are defined as those carrying L3 in any part of the body; mosquitoes harboring all other stages (mf, L1, and L2) are deemed infect*ed* (Goodman *et al.*, 2003). While it might be assumed that infected mosquitoes may become infective mosquitoes, the time span of at least two weeks (the approximate length of time it takes mf

to mature into L3 in the mosquito) is long enough that anything could happen to either the mosquito or filarial larvae and interrupt the possibility of infectivity. For example, in two weeks, the L1 or L2 in the gut of the mosquito may die. Epidemiologically, an accurate assessment of prevalence thus only includes those mosquitoes that are infective at any given time. Because non-larval stages (as well as the L4 stage) are never present in the mosquito vector, an appropriate transcript could also be present in those stages without compromising the integrity of a diagnostic assay for use in the vector.

Assessment of infection in vectors has advantages to monitoring the human populations after mass drug administration has been implemented in an endemic area (for example, the reluctance of human populations to submit to regular blood tests makes monitoring difficult) (Goodman *et al.*, 2003). The rapid and specific detection of mosquitoes carrying the infective stage larvae (L3) is an important component of the GPELF, and improved, sensitive and specific methods for detection continue to play a role in field diagnostics and in the monitoring of the elimination of lymphatic filariasis transmission (Ottesen, 2000).

The conventional method of assessment of infectivity in vectors has been manual dissection, with each dissector typically averaging thirty-five mosquitoes per hour (Bockarie *et al.*, 2000). PCR has been determined to be more sensitive for detecting filarial parasites than conventional, labor-intensive dissection and microscopy, and has already been used successfully when

monitoring onchocerciasis control programs (Yameogo *et al.,* 1999; Guevara *et al.,* 2003). An Ssp-I PCR assay for the monitoring of *W. bancrofti* prevalence has been developed in the Williams lab; however, standard DNA-based PCR assays cannot currently distinguish between infected mosquitoes and infective mosquitoes (Fischer *et al.*, 1999; Ramzy *et al*., 1997; Williams *et al.*, 2002b). The abundant larval transcript-2 (alt-2), an L3-upregulated gene that is the most highly-represented gene in the *B. malayi* L3 EST data set (3.5%), is initiated during development in the mosquito and declines sharply after the parasite has entered mammalian model host, making it a perfect candidate for an L3-specific RT-PCR diagnostic assay (Gregory *et al*., 2000). However, further evaluation of ALT-2 as a candidate has shown transcription initiated in the L2 stage, eliminating it as a prospect (Laney, personal communication). The identification of other possible targets would therefore be a useful contribution to the development of a diagnostic RT-PCR assay. An L3-stage specific transcript, perhaps a b20 splice variant, would be a valuable target for an RT-PCR assay to detect *infective* mosquitoes in endemic areas.

Very little is currently known about the function of b20 and its gene products. Identifying stage-specific splice variants, and characterizing the gene products of b20 in *B. malayi*, can contribute to an increased understanding of this gene and its possible role in larval development. The large number of presumed splice variants, as well as the lethal phenotype

evidence from *C. elegans*, suggest that it is a gene of some importance. Due to the previous plaque screenings of cDNA libraries suggesting a restricted developmental expression of Bmb20 forms to the L3 stage, Bmb20 may be most important during development from the L3 to L4 stage larvae, the first part of the life cycle that takes place in the human host (Walls, 2001). The successful identification and characterization of stage-specific splice variants in combination with the ongoing development of RNAi studies in *B. malayi* will allow RNAi studies specifically testing whether b20 knockdowns could prevent the molt from the infective L3 stage to the L4 stage of the parasite.

Because one of the goals for drug development is to prevent the parasite from establishing infection in the human host, such a b20 knockdown experiment could provide results relevant to the development of new drugs. RNAi experiments have been undertaken with some success in *B. malayi*. Previous experiments targeting β-tubulin or RNA polymerase III gave lethal phenotypes (as predicted), whereas disruption of the sheath protein shp-1 resulted in a mf sheath defect (Aboobaker and Blaxter, 2003).

Therefore, the importance of studying b20 in its own right as a gene whose function is as yet unknown is evident. Further evaluation and characterization of the different splice variant forms found in all the life cycle stages is an important step in this process. Additionally, exploiting one or more splice variants that might be found in the L3 stage may be useful in the

development of an RT-PCR assay for use in endemic areas as a method of detection of infective mosquitoes.

MATERIALS AND METHODS

Part I. RNA Extraction and cDNA synthesis

RNA was isolated from microfilaria (mf), L3, L4, adult female (AF) and adult male (AM) *B. malayi* worms obtained from the Filariasis Repository Research Service (Department of Medical Microbiology and Parasitology, The University of Georgia, Athens, GA). Subsequent to isolation from the gerbil host (mf, L4, AF, AM) or mosquito vector (L3), the parasites were washed in 1X PBS Buffer, quick frozen in liquid nitrogen, and stored at –80°C. RNA was isolated from *B. malayi* L1 and L2 six and eight days post infection obtained from the Department of Pathobiological Sciences of the School of Veterinary Medicine at Louisiana State University (Baton Rouge, LA).

For all RNA extraction procedures, care was taken to maintain an RNase/DNase-free environment. RNase-free certified tips and tubes were used. Bench top, pipettes and all equipment that was used was wiped with RNaseZAP (Ambion #9780) prior to use.

Worms were defrosted on ice, and, if stored in more than 250 μl of 1X PBS buffer, spun at 2500 rpm for 5 minutes at 4°C. Excess buffer volume was removed so that the starting volume of worms in solution was 250 μl. For

every 250 µl of worms in solution, 750 µl TRIzol LS (Invitrogen 10296-010) was added. Autoclaved 3 mm stainless steel beads were wiped with RNase-ZAP (Ambion #9780) and one bead was added to each tube. The tubes were vortexed at the highest speed possible for 30 minutes to facilitate homogenization of worm tissue. Every ten minutes, the tubes were rotated to ensure equal vortexing of all areas.

Chloroform (200 µl) was added (per initial 750 µl Trizol) to each tube, and the tubes were then vortexed for 15 seconds. The entire solution was transferred to pre-spun Phase Lock Gel Eppendorf tubes (#95515405), and maintained at room temperature for three minutes before being centrifuged at 4°C for 15 min at 12,000 x g. The aqueous phase was extracted into fresh microfuge tubes. The solution was kept on ice for all subsequent steps. If fewer than 200 larval worms were being used in the extraction, then 1 ul of 5µg/µl of glycogen was added prior to the addition of 500 µl of isopropanol (per initial 750 µl Trizol). The tubes were vortexed for approximately 15 seconds, placed at room temperature for 10 minutes and then centrifuged at 4°C for 10 minutes at 12,000 x g. The supernatant was removed, the pellet washed with 1 ml 75% ethanol (made with DEPC H2O), and then centrifuged at 4°C for 5 minutes at 7,500 x g. The supernatant was removed, the tube was inverted, and the pellet air-dried for 5 minutes. The RNA pellet was resuspended in 10-100 µl of RNase-free H2O, depending on yield (the relative size of the pellet obtained). For some extractions, the resuspended pellet was

placed in a 70°C incubator for 10-15 minutes after resuspension to facilitate resuspension of the pellet and prior to storage at -80°C.

The total concentration of extracted RNA was measured using the Nanodrop 3.0.1 spectrophotometer. 1 μl of RNA in 11μl of Northern Dye was run on an RNA gel (1.5% agarose in MOPS buffer) at approximately 86 volts for one hour to further evaluate the quality of the RNA.

cDNA was synthesized using Applied Biosystems TaqMan Gold RT-PCR Kit Protocol (N808-0234). According to the Applied Biosystems protocol, a 100 μl reverse transcriptase reaction will efficiently convert a maximum of 2 μg total RNA to cDNA. For the reverse transcription step, 1 μg of RNA was used in a 100 μl total reaction, except in cases where the RNA yield was substantially less (L1, L2). For those stages, the total amount of RNA extracted was used: 7.5 ng for L1, and 13 ng for both L2 day 6 and day 8. In the quantitative RT-PCR experiments in which this cDNA was used, the L2 day 6 and L2 day 8 cDNA samples were pooled. In addition to the RT-step being performed with the reverse-transcriptase enzyme, an RT-step without the reverse transcriptase enzyme (no-RT) was also carried out as a control for the quantitative RT-PCR step. For this reaction, the recipe was exactly the same with the difference in volume being made up with RNase-Free water.

For each 1 μg of template RNA, reverse transcriptase reactions were done using oligo d(T) primers. The protocol for this reaction is found in Appendix A. Subsequent PCRs were thus performed only on cDNA

constructed using the oligo d(T) primers, and all quantitative RT-PCRs were performed on oligo (dT)-constructed cDNA template. The RT step was performed in an Applied Biosystems Gene Amp PCR System 9700 with the following program specifics:

25°C	10 min
48°C	30 min
95°C	5 min
4°C	forever

All cDNA was stored at –20°C.

Part II: Primer Design and RT-PCR

Primers for non-quantitative PCR were designed using OLIGO 5.0 primer design program (an in-house primer design program in the Williams Lab at Smith College) and ordered from Integrated DNA Technologies (Coralville, Iowa). A list of the primers used in this evaluation can be found in Table 2 and in Figure 6. Primers were designed to the form-specific regions of the splice variant of interest. Because the RNA had not been treated with a DNase step (due to concerns about loss of quantity as well as possible degradation of the RNA following a DNase step) primers were designed to span an exon-exon junction to prevent amplification of any contaminating genomic DNA in the RNA sample. Additionally, primers spanned exon-exon boundaries because

that was the only way to ensure specific splice variants were being amplified. All primers were used at a working stock of 10 μM/μl and stored at -20°C.

With the goal of identifying and evaluating the expression pattern of b20 splice variants across the parasite life cycle, primers were first designed to constitutive exons flanking the most variable region of the gene (Figure 6). In addition, to search for a diagnostic candidate and to evaluate the expression pattern of individual splice variants across the life cycle, form-specific primers were used on mf, L3, L4, AF, and AM cDNA. Due to a paucity of parasite material for the L1 and L2 stages, this RNA was reserved for quantitative RT-PCR experiments.

Initially, 10 μl of 10 ng/100 μl cDNA was used for a total of 100 ng cDNA in PCR reactions. Successive experiments later used 5 μl of 1000 ng/100 μl cDNA (50 ng total) in all PCR reactions, with 5 μl more of RNase-free water being used to make up the accompanying difference in volume. The reaction mix used in all PCRs can be found in Appendix B. PCR reactions were run for forty cycles in an Applied Biosystems Gene Amp PCR System 9700 under the following conditions:

95°C	10 min	
54°C	30s	
72°C	45s	40 cycles
95°C	30s	
72°C	10 min	
8°C	forever	

PCR products were run on a 2% agarose gel at approximately 86 volts for at least one hour, though sometimes for as long as two and a half hours. PCR products resulting from the PCR using constitutive primers (amplifying a multitude of splice variants) were run on 4% agarose gels and for varying lengths of time (three to four hours) for better resolution. The gels were visualized using a UV light system subsequent to staining in ethidium bromide for five minutes followed two ten-minute destains in distilled water. All PCR products were stored at -20°C.

Table 1. b20 Splice Variant-Specific Primers Used in RT-PCR

Splice Variant/b20 form Being Tested	Primer Sequences (5' to 3')	Expected Size of PCR Product (bp)
Many (constitutive exons)	1071 F: ACAAAGGAAATTACGGGCTGC	Many (none greater than 983 bp)
	1072 R: TTACTTTTGGCTTCGCTGCA	
b20-I	1071 F: ACAAAGGAAATTACGGGCTGC	287
	1085 R: GCATATCACGTATTTGCTCATTTTTTG	
b20-j	1077 F: GGAAGACCAAAAAATGATGCT	375
	1074 R: TCGAGGCTTATCATCCTCAA	
b20-k	1073 F: TCCAGCTGCTGTTAAGAGTGA	202
	1074 R: TCGAGGCTTATCATCCTCAA	
B20-l	1077 F: GGAAGACCAAAAAATGATGCT	205
	1074 R: TCGAGGCTTATCATCCTCAA	
B20-n	1071 F: ACAAAGGAAATTACGGGCTGC	279
	1086 R: CCTCGAGGCTTATCATCATTTTTT	
Exon 91	1075 F: AAACGAAATGCTGGAACAACCT	85
	1076 R: CGTTGGACGATCTTCAAAAACA	
Exons preceding Exon 135	1071 F: ACAAAGGAAATTACGGGCTGC	394
	459 R: AGCTGGAACTGGTTCAGGTGC	
Exons preceding Exon 93	1071 F: ACAAAGGAAATTACGGGCTGC	394, 476
	394 R: GATCTGTCGGCTAAGTAAGT	
Exons preceding Exon 174	1071 F: ACAAAGGAAATTACGGGCTGC	394, 476, 647
	343 R: CAGCATTGGACCGGGAAAGGGTA	
B20-q	1071 F: ACAAAGGAAATTACGGGCTGC	279
	1108 R: TGTTTCTCACTATTTTTTGGTC	
B20-r	1071 F: ACAAAGGAAATTACGGGCTGC	370
	1107 R: GTTTCTCACTCGTAACATAA	

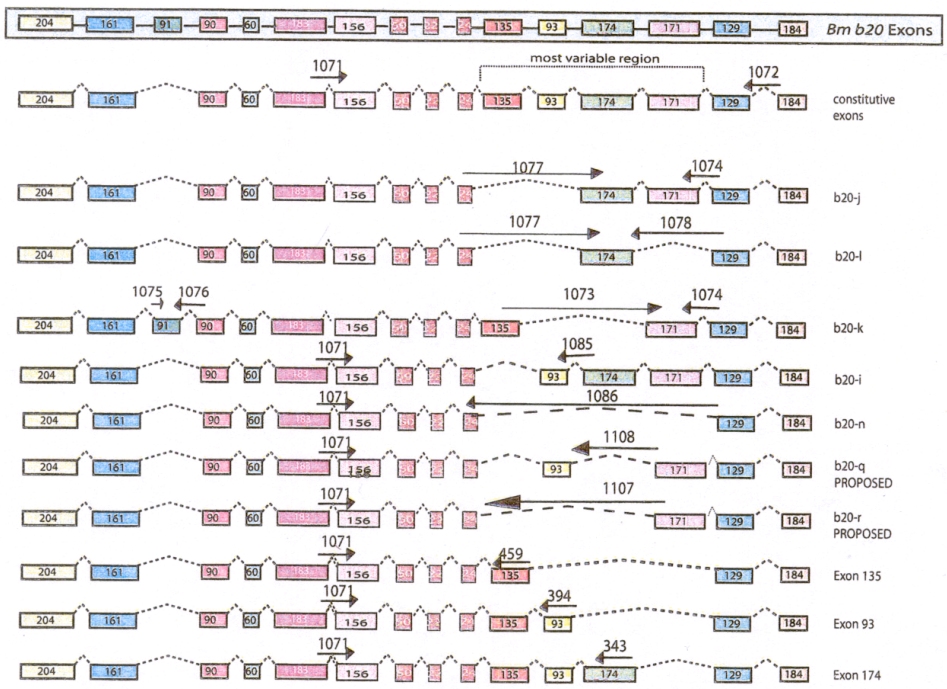

Figure 6. Schematic of Bmb20 splice variants to be characterized in RT-PCRs. Each splice variant is specific due to a particular exon splicing pattern shown in the above figure. Primers specific to each splice variant were designed to span exon-exon boundaries and are shown above each splice variant.

Part III: Quantitative RT-PCR

Signal strength by agarose gel detection was used to select two splice variant candidates that might potentially be upregulated in the L3 stages as compared to the other life cycle stages. These two splice variants, b20-l and b20-n, were evaluated by quantitative RT-PCR to further characterize the differential expression of those splice variants relative to life cycle stage. Quantitative RT-PCR quantifies product as it accumulates during the exponential phase of amplification, where the threshold cycle (Ct) value is defined as the number of PCR cycles required for the fluorescence signal to exceed the background fluorescence.

Nucleoside Diphosphate Kinase (NDK) was previously selected and used as an endogenous control for RT-PCR studies concerning *B. malayi* (Saunders, 2000). Because this primer and probe set was not initially designed with regard to exon-exon boundaries, new primers that did span exon-exon boundaries were designed using ABI PrimerExpress software, Version 1.0, to flank the already-available probe sequence and ordered from Integrated DNA Technologies (Coralville, Iowa). Two other primer and probe sets were also designed using the Primer Express software to test the relative levels of expression of b20-l and b20-n. As opposed to the non-quantitative RT-PCR,

where the *primers* were specific for the splice variant form being amplified, the *probes* used in qRT-PCRs were specific for the splice variant form, and flanked the relative exon-exon boundaries specific to the b20-l and b20-n formes being tested. All probes were ordered from ABI Prism (Foster City, CA) and primers were ordered from Integrated DNA Technologies (Coralville, Iowa). A minus RT control reaction was done to ensure that amplification was not occurring due to any possible genomic DNA (gDNA) contamination in the RNA. In order to further validate that any contaminating gDNA from the RNA isolation step was not amplified by the primers designed for use in quantitative RT-PCR experiments, PCRs using these primers were run on L3 cDNA and visualized on a 2% agarose gel (Figure 7). Refer to Table 2 for all primer and probe sequences used in quantitative experiments.

All probes were used at a concentration of 250 nM, per the specifications of Applied Biosystems. Both forward and reverse primers were optimized with varying combinations of the following concentrations: 50 nM, 300 nM, and 900 nM. Primer optimization studies were completed using 10 ng and 1 ng of template cDNA. From those primer optimization reactions, the combination of forward and reverse primer concentrations that indicated the greatest reproducibility as well as the lowest Ct value (cycle number) and highest relative delta Rn (fluorescence) for NDK, b20-n, and b20-l were chosen as primer concentrations to be used in experiments. For the NDK, the optimal concentrations of forward and reverse primers was found to be 50 nM

for the forward, and 300 nM for the reverse. For both b20-l and b20-n, the optimal concentrations for both the forward and reverse primers was determined to be 900 nM (Table 3).

Table 2. Primers and Probes used in Quantitative RT PCR Experiments

Gene	Role of Gene	Probe Sequence (5'VIC - TAMRA3')	Primer Sequences (5'-3')
NDK	Endogenous Control	TTCCTTGCCTTCAGCCGAACGTG	F: CCTCTAAATTCAATGCCAGGTACTAT
			R: CACTCACAGAGTTCTTCTGGTTTAA
B20-l	Target; unknown	ACTGCGCACATTGAGGATGATAAGCCTCGT	F: GGAAGACCAAAAAATGATGCTTC
			R: GCTCACGACGCTTCATAATACC

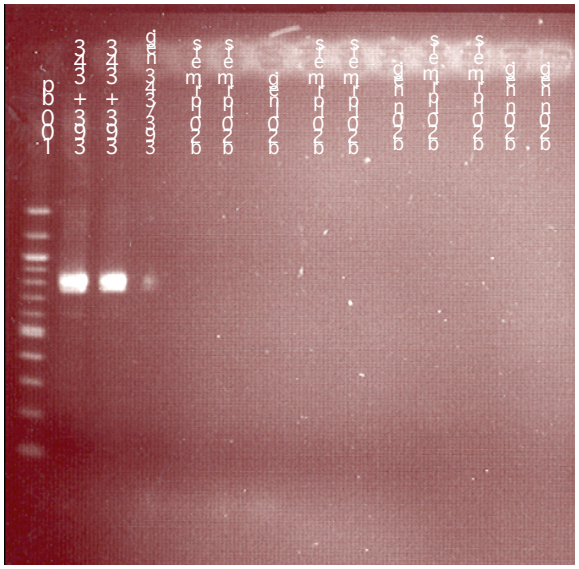

Figure 7. Photograph of PCR products resulting from PCRs done on *B. malayi* genomic DNA with specific b20-l (F 1103, R 1104), b20-n (F 1105, R 1106), and NDK (F 1125, R 1126) primers designed for use in qRT-PCR. These primers were designed across exon-exon boundaries to prevent amplification of any genomic DNA contamination in the cDNA template for qRT-PCR. This PCR, done on genomic DNA, was to verify that all primers to be used in qRT-PCR specifically amplified only cDNA. The PCR product in Lanes 2 and 3, labeled 393/343, was a PCR done on genomic DNA but with a previously designed primer set that spanned introns, thus ensuring genomic DNA would be amplified. The presence of a band of the predicted PCR size (800 bp) indicates that genomic DNA was amplified. The lack of any PCR products in all other lanes indicates that the specific qRT-PCR primers designed for b20-l, b20-n, and NDK did not amplify any contaminating genomic DNA in any reactions.

Table 3. Optimized Concentrations of Primer and Probes used in qRT-PCR

Gene	Role of Gene	Concentration of Probe (nM)	Concentration of Primers (nM)	
NDK	Endogenous Control	250	F# 1125	50
			R # 1126	300
b20-l	Target; unknown	250	F # 1103	900
			R# 1104	900

The qRT-PCR experiment was designed to test the relative quantification of the designated targets, splice variants b20-l and b20-n. Relative quantification describes the change in expression of a particular target relative to some reference group (in this case, chosen to be the mf for data analysis). The relative standard curve method was used to compare the expression of the b20 splice variants relative to life cycle stage because it was determined that the efficiencies of the target reactions (b20-l and b20-n) were not similar to the efficiency of the NDK reaction as determined by dilution curves (data not shown). All quantitative RT-PCR experiments were performed and analyzed using the ABI PRISM 7700 Sequence Detection System. Relative standard curves for each primer and probe set (b20-l, b20-n, and NDK) were constructed using seven ten-fold dilutions of template (Figures 8 and 9). The template used for the NDK standard curve was PCR product from a PCR using NDK qRT-PCR primers 1125 and 1126 on the L3 cDNA library. The template used for the b20-l and b20-n standard curves was PCR product resulting from a PCR done on L3 cDNA using primers 1071 and 1072 designed to constitutive b20 exons. All PCR products were purified using Qiagen PCR purification columns (# 28104; Qiagen Inc, Valencia, CA) according to manufacturer instructions. The quantitative RT-PCR reactions

used to construct the standard curve were performed under the same conditions as experimental quantitative PCRs; 250 nM of probe was used in each respective reaction and the optimal primer concentrations as previously determined were used in each separate PCR. For each primer and probe set, the average Ct value of the replicates was used to construct a standard curve of Ct vs. log Total Amount of PCR Product Template used in the reaction (Figures 8 and 9). However, it was impossible to construct an accurate relative standard curve for the b20-n splice variant. Amplification started at very high Ct values, suggesting that this splice variant is present only at a very small amount (nearly undetectable). Therefore, b20-n was no longer considered a good candidate to be evaluated using quantitative RT-PCR, and the quantitative RT-PCR study was limited to the b20-l splice variant.

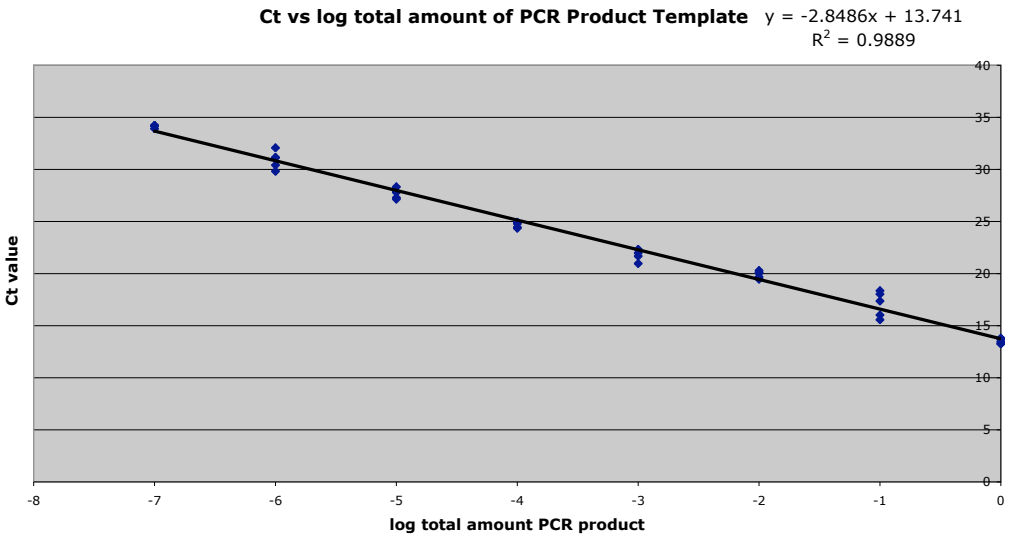

Figure 8. NDK standard curve generated using PCR product resultant from a PCR amplifying from a L3 *B. malayi* cDNA library with NDK qRT-PCR primers (1125 and 1126). The curve was used for analysis of qRT-PCR results.

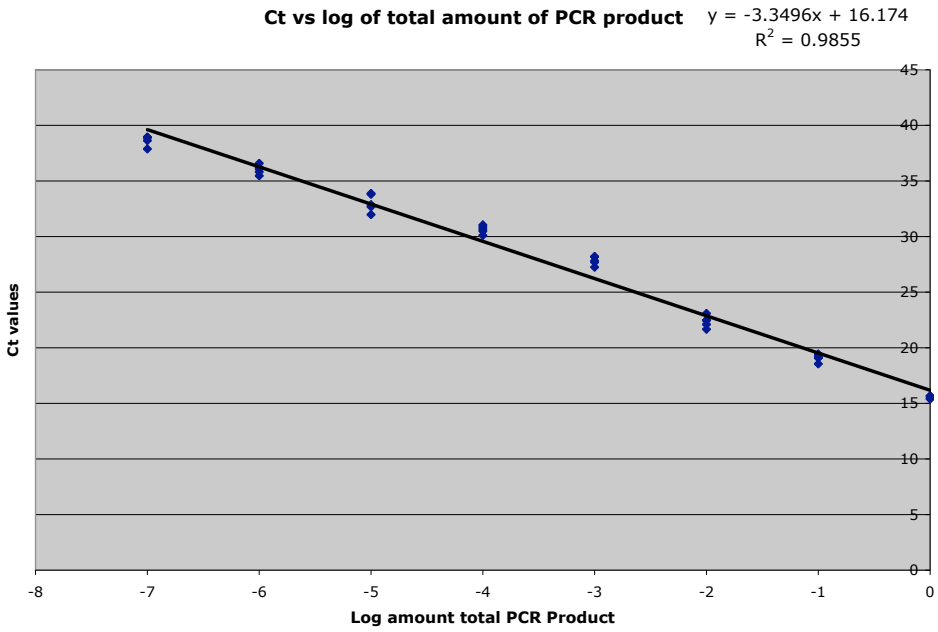

Figure 9. b20-l standard curve generated from PCR product resulting from a PCR on L3 cDNA with primers designed to constitutive exons 183/156 and 129/184 (primers 1071 and 1072). The curve was used for analysis of qRT-PCR results.

The quality of the NDK and b20-l standard curves can be determined from their slope and correlation coefficients (R^2). After constructing the standard curve, quantitative PCR testing for the expression of b20-l was performed in triplicate on 1 ng of Oligo d(T) cDNA template from each life cycle stage of *B. malayi*: mf, L1, L2, L3, L4, AF and AM. Quantitative PCR was also performed in triplicate on 10 ng of Oligo d(T) cDNA from the mf, L3, L4, AF and AM life cycle stages of *B. malayi*. The L1 and L2 could not be tested at that quantity due to lack of parasite material. Refer to Appendix C for reaction recipes used in the quantitative RT-PCRs. PCR reactions were run for forty cycles in the ABI PRISM 7700 Sequence Detection System under the following conditions:

50°C	2 min	
95°C	10 min	
95°C	15 s	
60°C	1 min	40 cycles

The average Ct values for each set of triplicates was used with the standard curve to evaluate relative levels of expression of the target splice variant of interest, b20-l, in all life cycle stages of *B. malayi*, with the mf stage

serving as the calibrator (the life cycle stage against which all others are compared to).

RESULTS

Part I. RNA Extraction

RNA was isolated from mf, L1, L2, L3, L4, AF, and AM *B. malayi* worms (Figure 10). RNA yields varied dependent on the life cycle stage of extraction and are summarized in Table 4 as measured by spectrophotometry.

Part II. RT-PCR Evaluation of Bmb20 Splice Variant Expression

A. Overall splice variant expression

Data from previous plaque screens of *O. volvulus* cDNA libraries showed that the exons 183, 156, 129 and 184 were constitutively expressed b20 exons (present in all cDNA transcripts). Therefore, forward primer 1071 and reverse primer 1072, designed across the junctions of constitutive exons 183/156 and 129/184, and flanking the variably spliced exons, should amplify all splice variants expressed. The expected size range of PCR products was 410 bp to 983 bp (Table 5), as predicted by splice variants previously identified in *O. volvulus* (Figure 4). When visualized on a 4% agarose gel, a large number of PCR products, ranging in size from 518 bp to 983 bp were visible (Figure 11). Additionally, at least two bands at approximately 716 bp,

750 bp and 900 bp, not present in any of the other stages, indicate the possibility of L3-specific splice variants of Bmb20.

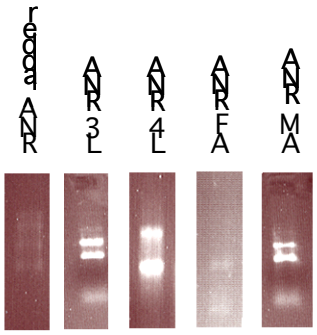

Figure 10. Photographs from representative gels indicating the quality of RNA used to synthesize cDNA for use in later RT-PCR experiments. Amounts of RNA run on quality-check gels ranged from 50 ng to 200 ng (L4 = 50 ng, AF = 150 ng, L3 and AM = 200 ng).

Table 4. RNA Extraction Yields (μg) from *B. malayi* Life Cycle Stages

Stage/starting number of worms	Mf: $1x10^6$ worms	L1 180 worms	L2 630 worms	L3 3000 worms	L4 500 worms	AF 6 worms	AM 52 worms
RNA extracted (μg)	22	0.074	0.12	12.65	9.8	9.8	11.2

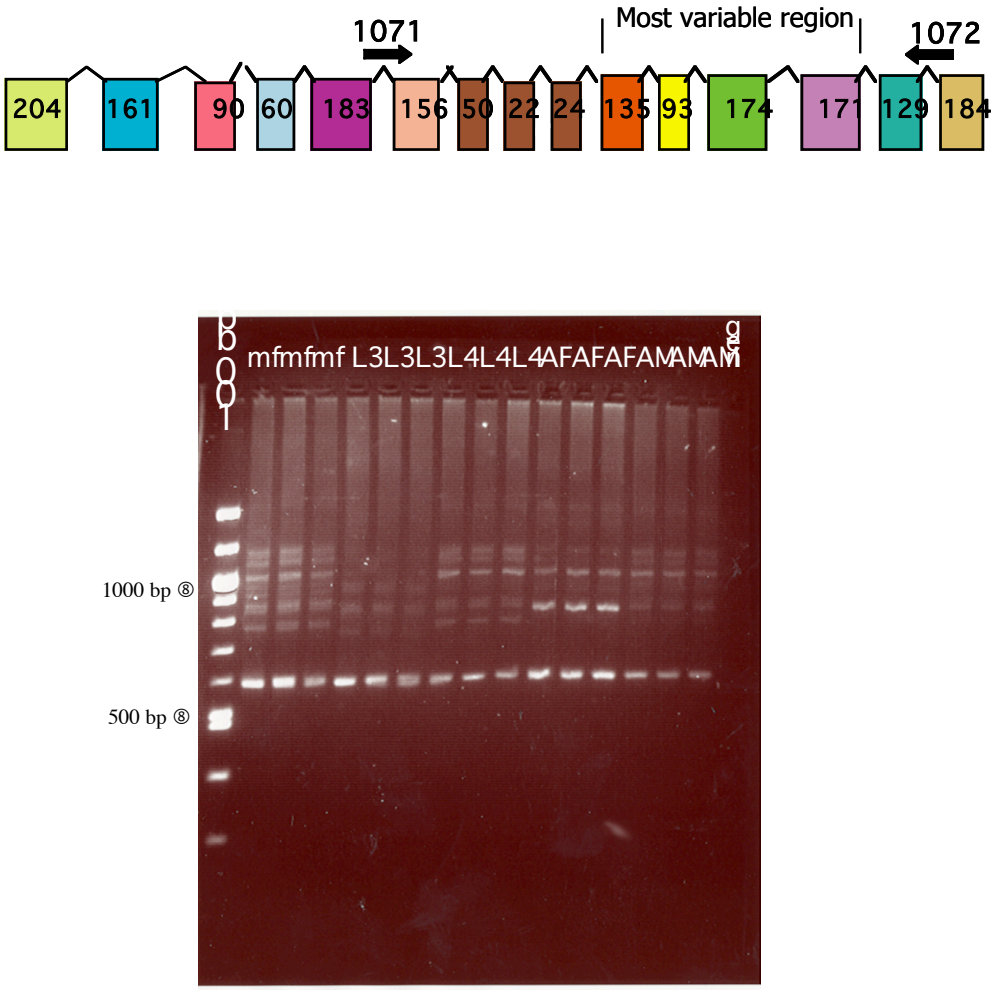

Figure 11. Photograph of PCR products run on a 4% agarose gel for six hours at approximately 60 volts, from a PCR using forward primer 1071, spanning the exon boundary of constitutive exons 183 and 156, and reverse primer 1072, spanning the exon boundary of the constitutive exons 129 and 184. The PCR was performed on *B. malayi* mf, L3, L4, AF, and AM cDNA template. The largest possible PCR product predicted from using these primers was 983 bp. The largest PCR products observed are greater than 1000 bp, suggesting that perhaps nonspecific priming occured. Multiple PCR products, representing multiple individual splice variants, are present in all of the life cycle stages tested, thus complicating sequencing efforts that would further characterize these variants. While the reproducibility of this photograph may make it difficult to see, there are at least three L3-specific bands of approximate sizes 716, 750 and ~900 bp.

Table 5. PCR Products Resulting from the PCR done with Primers 1071 and 1072

Sizes expected (bp)	Sizes Detected (bp)	Stage of Detection
410	None	None
581	581	all
584	None	None
	610	L3
	650	mf, L3
	680	L3
716	716	L3
	~ 750	L3
755	755	L3, L4, Af, AM
812	812	all
848	848	all
890	890	all
	900	L3
983	983	all

B. Splice variant-specific RT-PCR

In order to evaluate the expression pattern of b20 splice variants, RT-PCR experiments were done using primers designed to splice variant-specific regions of the b20 gene on parasite RNA from each of these stages: mf, L3, L4, AF and AM. The L1 and L2 stages of the parasite were not evaluated in this part of the study due to the difficulty in obtaining sufficient quantities of L1 and L2 worms and thus RNA. Splice variants b20-i, b20-j, b20-k, b20-l, b20-n, b20-q, and b20-r were the specific splice variant forms tested (Table 6).

No stage-specific expression of b20 forms i, j, k, q or r

Previous plaque screens of *O. volvulus* and *B. malayi* L3 cDNA libraries suggested that the splice variants b20-j, b20-k, and b20-i were expressed in a stage-specific manner in both nematodes. Agarose gel electrophoresis of PCR products from the PCR tests of *B. malayi* cDNA with primers designed to the form-specific regions of b20-i, b20-j, and b20-k showed the absence of any stage-specific expression of these alternatively-spliced forms in *B. malayi*.

The b20-i splice variant was detected in all life cycle stages (Figure 12). The presence of b20-i was tested with forward primer 1071, spanning exons 183 and 156, and reverse primer 1085, spanning exons 93 and 174. The presence of a PCR product of the predicted size of 287 bp in all life cycle stages indicates b20-i is not regulated in a stage-specific manner.

The b20-j splice variant was detected in all life cycle stages in a PCR performed with forward primer 1077, spanning exons 24/174, and reverse primer 1074, spanning exons 171/129. Because of sequence similarity at the exon junctions of exons 171/129 and 174/129, the reverse primer 1074 also amplified the b20-l splice variant in this PCR. Though reverse primer 1074 amplified both b20-j and b20-l in the same reaction, the two splice variants could be easily differentiated by size (Figure 13). PCR products of 202 bp, the predicted size of the b20-l variant, are visible in some life cycle stages, and PCR products of 375 bp, the predicted size of the b20-j variant, are present in all life cycle stages. The clear presence of the PCR product of 375 bp in all life cycle stages indicates that b20-j is not L3 specific.

The b20-k splice variant was tested with forward primers 1073, spanning exons 135/171 and reverse primer 1074, spanning exons 171/129. A band of 202 bp, the size of the predicted PCR product, is present in all life cycle stages (Figure 14). Because of the lack of any detectable bands, in addition to the lack of 'schmear' in the L4 lanes, it is possible that no L4 template was added to those samples prior to the PCR. Due to the relative intensity of the band found in the L3 lanes, it is possible that there may be a relatively higher level of expression of PCR product in that life cycle stage relative to others. However, the distinct presence of the b20-k form-specific region in all life cycle stages, except for L4, showed that b20-k was not stage-specific with regard to expression.

Because of the presence of L3-specific bands from the initial PCR done with the constitutive exons, two splice variants, never previously identified in either *B. malayi* or *O. volvulus*, were hypothesized. Designated b20-q and b20-r, these proposed splice variants are of the same approximate size as those unknown L3-specific bands visible on the constitutive PCR gel. The b20-q and b20-r form-specific regions were artificially constructed using proposed hypothetical exon combinations that might explain the possible splice variants responsible for the L3-specific bands of approximate size 750 bp detected in the PCR done with constitutive exons. The b20-q form was designated to be a splice variant with a form-specific region consisting of exon 124 directly spliced to exons 171 (Figure 6). The b20-r form was designated to be a splice variant with a form-specific region consisting of exon 93 directly spliced to exon 171 (Figure 6). Primers were designed to these hypothetical exon arrangements and PCR products of the predicted sizes for both of these potential forms were identified in all life cycle stages. However, verification by sequencing of the PCR product has not yet occurred. Therefore, it cannot be confirmed at this time that the PCR products are the proposed splice variants. Whatever splice variants these PCR products do represent, neither are expressed in a stage-specific manner (Figures 15 and 16).

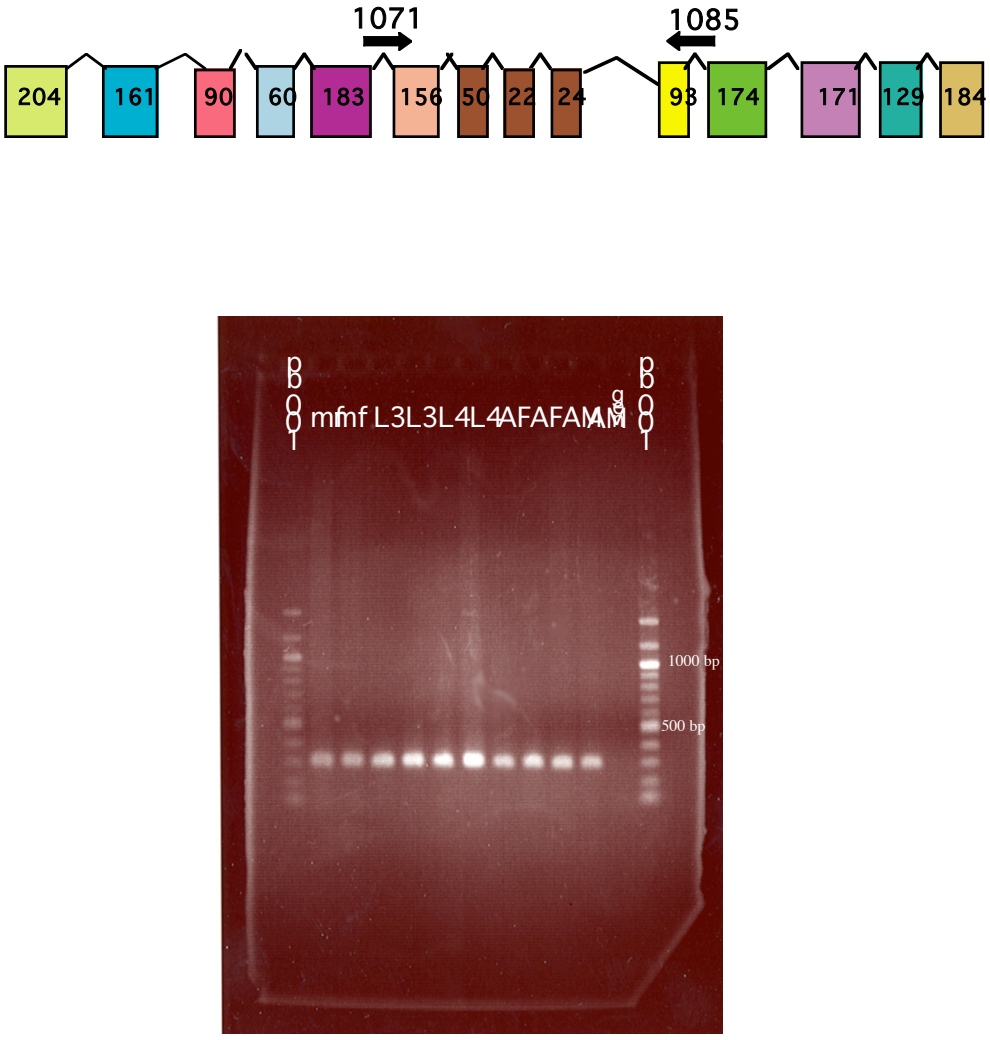

Figure 12. Photograph of PCR products, run on a 2% gel for 1 hour at 86 V, from a PCR testing for the form-specific region of the b20-i splice variant in all life cycle stages. Forward primer 1071, spanning the exon boundary of constitutive exons 183 and 156, and reverse primer 1085, spanning the exon boundary between exons 93 and 174, were used in this reaction, with the PCR performed on mf, L3, L4, AF, and AM cDNA. The size of the predicted PCR product for this reaction was 287 bp, and this gel clearly shows the presence of a band of approximate size 287 bp in all life cycle stages tested. Therefore, splice variant b20-i is not expressed in a stage-specific manner in *B. malayi*.

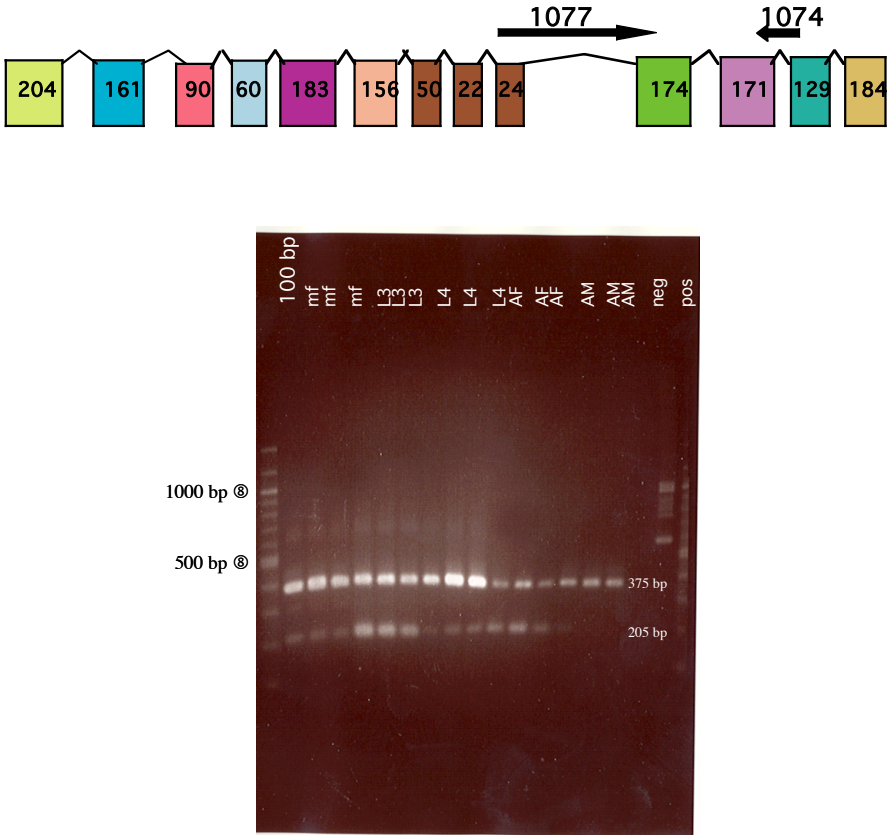

Figure 13. Photograph of PCR products, run on a 2% gel for 1 hour at 86 V, from a PCR testing for the form-specific region of the b20-j splice variant. Forward primer 1077, spanning the exon boundaries of exons 24/174, and reverse primer 1074, spanning exon boundaries 171/129, were used in this reaction, with the PCR performed on mf, L3, L4, AF and AM cDNA. Two PCR products were observed in the mf, L3, L4, and AF life cycle stages, with one band of size 375 bp and the other band of approximately 200 bp. This 375 bp band corresponds to the predicted size of the PCR product for the form-specific region of b20-j, while the smaller corresponds to the predicted size of the PCR product for the b20-l splice variant. Because the 375 bp product of the form-specific region of b20-j are present in all life cycle stages tested, with suggested upregulation in larval stages according to signal intensity, it is clear that b20-j is not expressed in a stage specific manner in *B. malayi*.

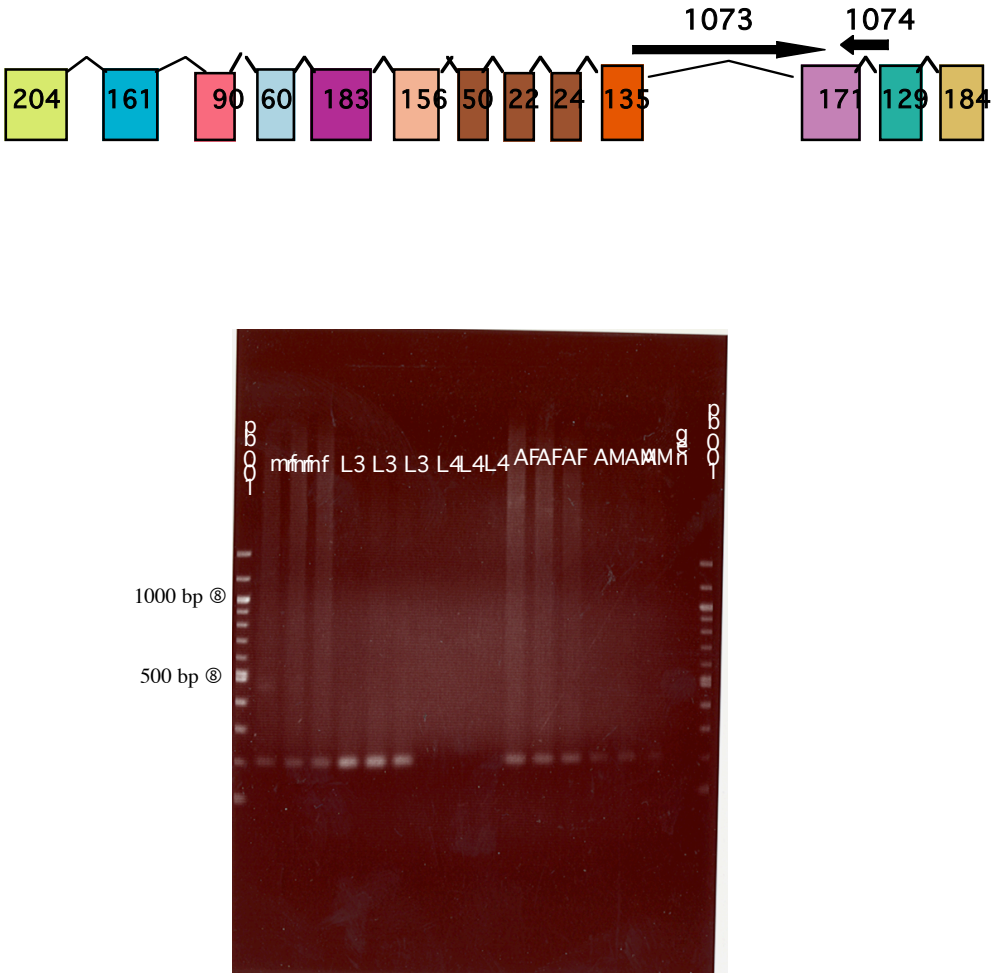

Figure 14. Photograph of PCR products, run on a 2% gel for 1 hour at 86 V, from a PCR testing for the form-specific region of the b20-k splice variant. Forward primer 1073, spanning the exon boundaries of exons 135 and 171, and reverse primer 1074, spanning exon boundary between exons 171 and 129, were used in this reaction. The size of the predicted PCR product is 202 bp, and a band of 202 bp is present in all replicates for all stages, except for the L4 stage. Due to the notable lack of a 'schmear' indicating any PCR product in the L4 lanes, it is possible that no L4 template was added to this reaction. There appears to be a more intense signal detection of the b20-k form in the L3 stage as compared to the other stages. Due to the presence of PCR product in all stages (except L4) however, b20-k is not expressed in a stage-specific manner in *B. malayi*.

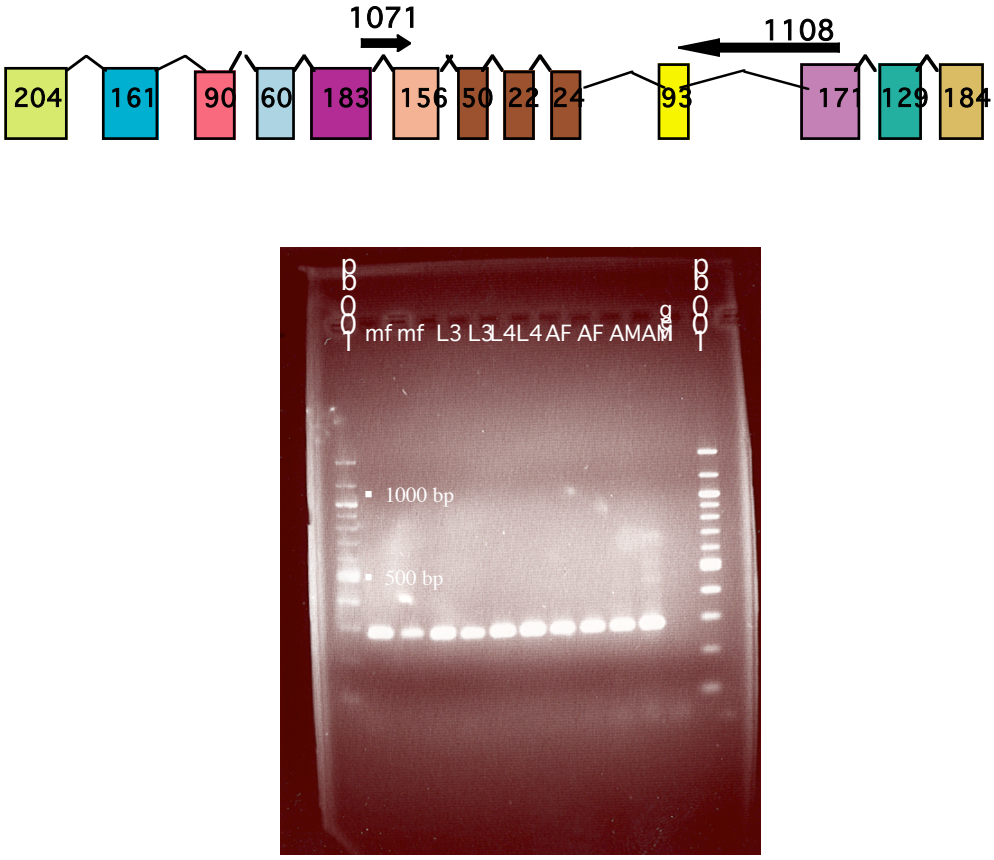

Figure 15. Photograph of PCR products, run on a 2% gel for 1 hour at 86 V, from a PCR testing for the form-specific region of the proposed b20-q splice variant in all life cycle stages. Forward primer 1071, spanning the exon boundary of constitutive exons 183 and 156, and reverse primer 1108, spanning the exon boundary between exons 24 and 171, were used in this reaction, with the PCR performed on mf, L3, L4, AF, and AM cDNA. The size of the predicted PCR product for this reaction was 279 bp, and this gel clearly shows the presence of a band of approximate size 279 bp in all life cycle stages tested, indicating this splice variant is not expressed in a stage-specific manner. Though a PCR product of the expected size for b20-q was obtained, without sequencing the product, it cannot be determined that this PCR product does in fact represent the sequence/exon pattern of the proposed splice variant b20-q.

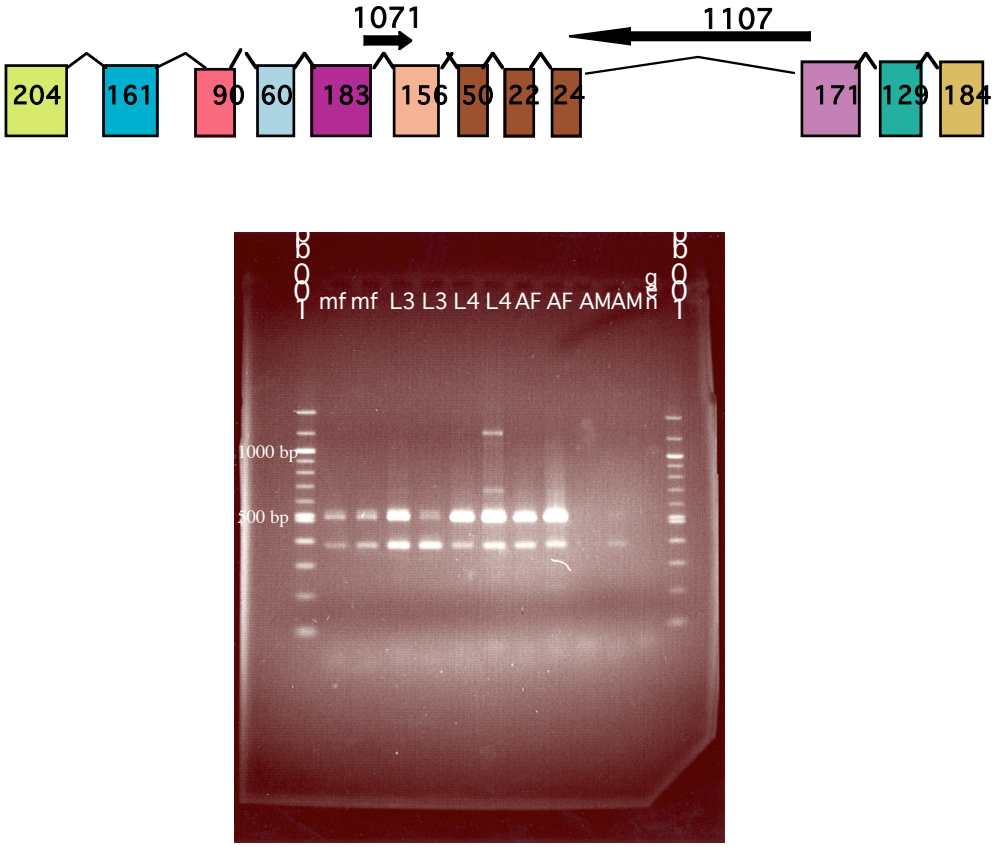

Figure 16. Photograph of PCR products, run on a 2% gel for 1 hour at 86 V, from a PCR testing for the form-specific region of the proposed b20-r splice variant in all life cycle stages. Forward primer 1071, spanning the exon boundary of constitutive exons 183 and 156, and reverse primer 1107, spanning the exon boundary between exons 93 and 171, were used in this reaction, with the PCR performed on mf, L3, L4, AF, and AM cDNA. The size of the predicted PCR product for this reaction was 370 bp, and this gel clearly shows the presence of a band of approximate size 370 bp in all life cycle stages tested, except for the AM. There is a faint band of the appropriate size in only one of the AM replicates, perhaps suggesting that this splice variant is expressed at a very low level in the AM stage. The presence of another band, at approximately 520 bp, indicates an instance of nonspecific priming. Because a PCR product of the expected size was present in multiple life cycle stages, this variant is not expressed in a stage-specific manner. Though a PCR product of the predicted size for b20-r was obtained, without sequence data, it cannot be determined that this PCR product actually represents the proposed splice variant b20-r.

b20-l and b20-n variants may be upregulated in L3

The PCR tests of two specific splice variants, b20-l and b20-n, suggested their upregulation in the L3 stage as compared to the other life cycle stages. b20-l is a splice variant previously identified in *O. ochengi* L3, and b20-n was previously identified in *O. volvulus* L3. The PCR test for the b20-l splice variant done with forward primer 1077 and reverse primer 1074 resulted in a PCR product of the predicted size, 205 bp, present in all life cycle stages. However, the relative intensity of the band in the L3 as compared to the other life cycle stages suggested possible upregulation of b20-l in L3 (Figure 17).

The PCR test for the b20-n splice variant, using forward primer 1071 and reverse primer 1086, resulted in the detection of the predicted PCR product of 279 bp in all life cycle stages, with a single PCR product of predicted size 279 bp in the mf, L3, L4 (only one lane positive), AF and AM (though two other PCR products, of size 200 bp and approximately 700 bp, were also amplified in the AF stage). The relative intensity of the 279 bp band in the L3 stage as compared to the other life cycle stages suggested that there may be possible upregulation of the b20-n splice variant in the L3 form relative to the other life cycle stages, though it is not restricted exclusively to the L3 stage (Figure 18).

Therefore, signal strength by agarose gel detection of PCR products from PCR tests of *B. malayi* cDNA with primers designed to the form-specific regions of b20-l and b20-n suggested the relative upregulation of these splice variants in the L3 stage as compared to the other stages. Because no L3-

specific splice variants had been identified, these two splice variants were chosen as good candidates for further evaluation of relative levels of expression using quantitative RT-PCR.

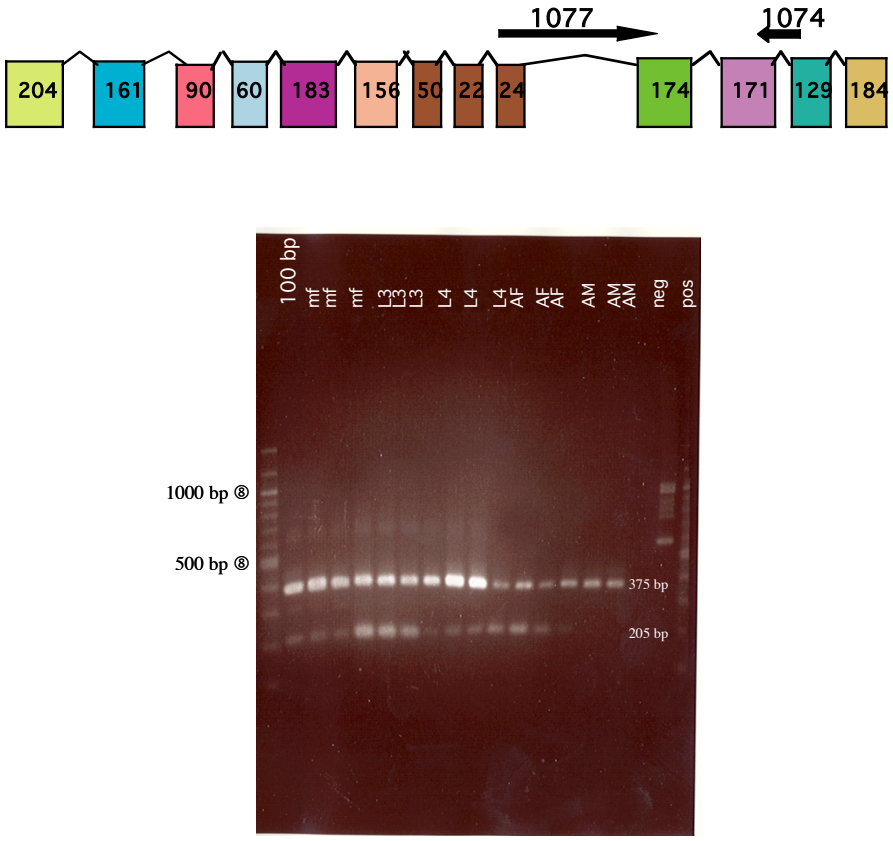

Figure 17. Photograph of PCR products, run on a 2% gel for 1 hour at 86 V, from a PCR testing for the form-specific region of the b20-l splice variant. Forward primer 1077, spanning the exon boundaries of exons 24 and 174, and reverse primer 1074, spanning exon boundaries 171 and 129, were used in this reaction on mf, L3, L4, AF and AM cDNA. Two PCR products are present in the mf, L3, L4, and AF life cycle stages, with one band of size 375 bp and the other band of approximately 200 bp. This 375 bp band corresponds to the predicted size of the PCR product for the form-specific region of b20-j, while the smaller band corresponds to the predicted size of the PCR product for the b20-l splice variant, 205 bp. The 375 bp product of the form-specific region of b20-j is present in all life cycle stages tested. The 205 bp product of the form-specific region of b20-l appears to be present at some level of expression in the mf, L3, L4, and AF stages, with a relatively less intense detection signal in all stages compared to the L3, indicating that there may be upregulation of b20-l in the L3 stage.

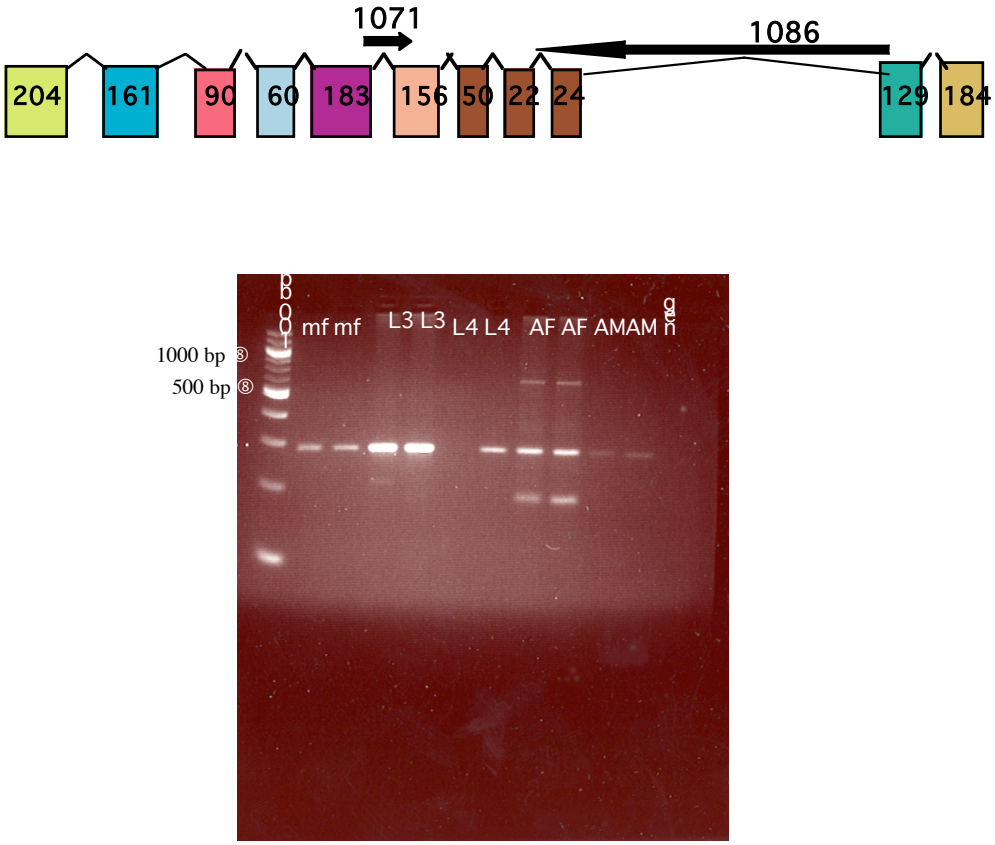

Figure 18. Photograph of PCR products, run on a 4% gel for 1 hour at 86 V, from a PCR testing for the form-specific region of the b20-n splice variant in all life cycle stages. Forward primer 1071, spanning the exon boundary of constitutive exons 183/156, and reverse primer 1086, spanning the exon boundary between exons 24/129, were used in this reaction, with mf, L3, L4, AF and AM cDNA. The predicted size of this PCR was 279 bp, and a band of this size is present in all life cycle stages on this gel, though only faintly in the mf and very faintly in the AM, and one of the two replicates of the L4 stage shows no band. However, there appears to be upregulation of this form specific region in the L3 as compared to the mf. There also appears to be a high level of expression in the AF, in addition to a second PCR product of smaller size (~ 200 bp) than predicted, as well as a PCR product of a larger size (~700 bp) than predicted in the AF stage. These are probably instances of non-specific priming. However, the very strong signal detection of the predicted PCR product for the b20-n splice variant indicates that it may be upregulated in the L3 stage.

Table 6. Bmb20 Splice Variants Identified by RT-PCR

Splice Variant Form	Stage of Expression	Possible Stages of Upregulation
b20-i	All	L4?
b20-j	All	Mf, L3, L4
b20-k	mf, L3, AF, AM	L3?
b20-l	All (very low in AM)	L3, AF?
b20-n	All (very low in AM)	L3, AF
Proposed b20-q	All	Highly expressed in all
Proposed b20-r	All (very low in AM)	L3, L4, AF

C. Specific Exon PCR

Previous plaque screening experiments with *O. volvulus* cDNA libraries had indicated that exon 91 was expressed in a stage specific manner, found only in the splice variant b20-k, present in the molting L3 stage (L3M) (Figure 4). Agarose gel electrophoresis of PCR products from a PCR using *B. malayi* cDNA with forward primer 1075 and reverse primer 1076, designed to amplify exon 91, showed the presence of the predicted PCR product of 85 bp in all life cycle stages (Figure 19). Though the expression of this exon has been detected in all *B. malayi* lifecycle stages, this PCR experiment did not address its expression with regard to which particular splice variant forms in which it might be present. While its presence in each life cycle stage has been determined, the splicing pattern of this exon is still unknown. No further experiments were performed at this time to determine its place in the splicing pattern of Bmb20.

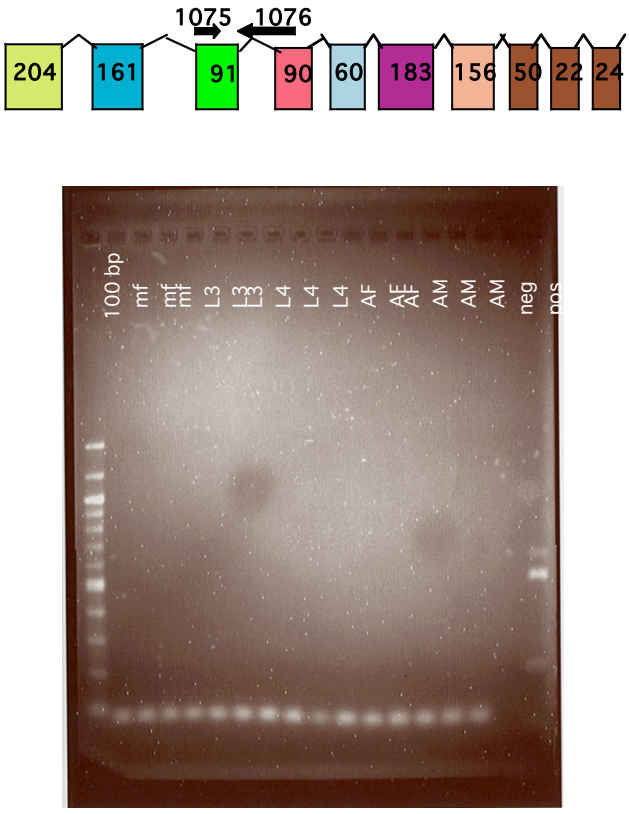

Figure 19. Photograph of PCR products, run on a 2% gel for 1 hour at 86 V, from a PCR testing for the presence of exon 91 in all life cycle stages. Previous studies found that the *O. volvulus* exon 91a was expressed only in the L3 stage. Forward primer 1075, specific for a sequence within exon 91, and reverse primer 1076, spanning the exon boundary between exons 91 and 90 were used in this reaction on mf, L3, L4, AF, and AM cDNA. A PCR product of the expected size, 85 bp, is present and expressed in all life cycle stages of *B. malayi*. Though the exon is present in all life cycle stages, its particular expression pattern with regard to alternatively spliced forms is still unknown. Though the results of this experiment thus suggest that exon 91 is expressed in every life cycle stage, the specific forms it is found in are still unknown. The main result of this experiment illustrates that, unlike what was previously found in *O. volvulus*, this exon is *not* expressed in a stage-specific manner.

D. Search for additional exons

The *B. malayi* genome was sequenced in April 2004 (Ghedin et al, 2004), but there remains a lack of genomic information concerning the region of Bmb20 where the exons 50, 22, and 24 are located (Figure 5). Previous data from the same region in Ovb20 (Figure 4) suggested the constitutive expression of the exons in that region, and this was assumed to be the case with Bmb20 as well. The results of the initial PCR done with primers to constitutive exons indicated L3-specific bands in the unpredicted size range of 600 to 700 bp (Table 5), suggesting the possibility that these bands could be due to the presence of additional, unknown exons. The only region for which genomic data is not available, and therefore in which extra exons would be found in Bmb20, is the 50-22-24 exon region.

In order to test the hypothesis that there may be extra exons in this region, three different PCR experiments were performed. Forward primer 1071, spanning the exon boundary of constitutive exons 183 and 156 was used in all three reactions. Specific reverse primers 459, 394, and 343 were designed to sequences within exons 135, 93, and 174 respectively (Figure 20). Exons 135, 93, and 174 are immediately downstream of the 50-22-24 region. If no extra exons are present in this region of the gene, there should be only a certain number of PCR products possible. For example, only one PCR product should result from the PCR with reverse primer 459 designed to exon 135, two products are expected from PCR testing exon 93 (the product of exon 24

spliced with 135, as well as exon 24 spliced with 93) and three PCR products are expected from the PCR testing exon 174. The number of possible products increases with each successive downstream exon, because not only will the PCR product containing just that exon be amplified, but also the PCR products of that exon spliced with all known upstream exons included in the region. However, if there are extra exons present in the 50-22-24 region, then *more* PCR products than expected would result from each of these experiments.

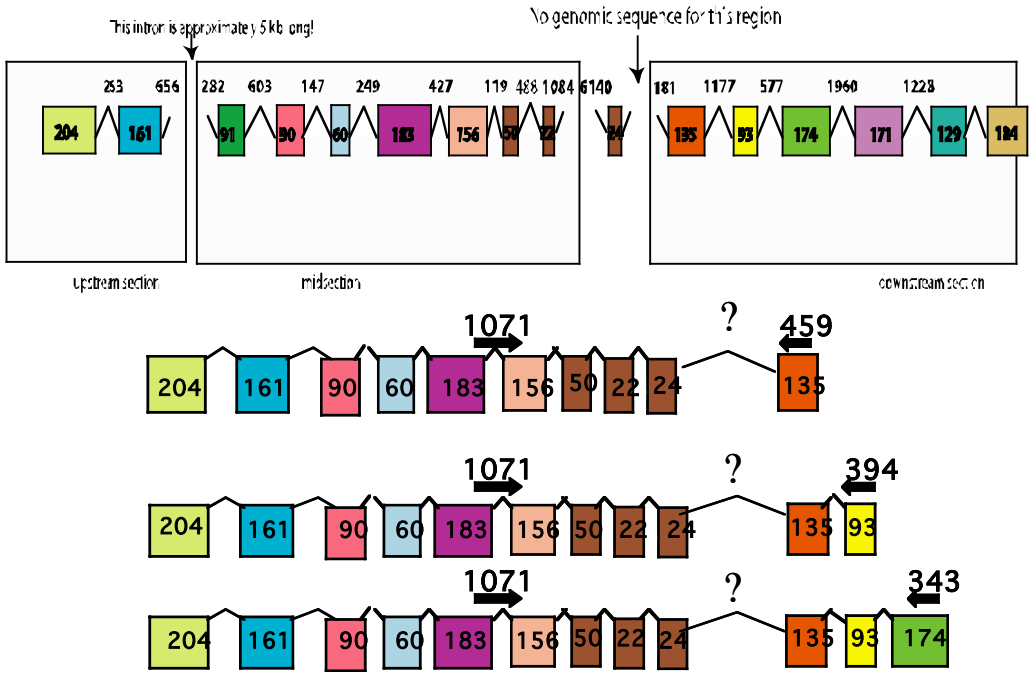

Figure 20. Schematic diagram of the PCR experiments designed to test for the presence of potential additional exons in the 50-22-24 region of the b20 gene. Shown at the top is the current genomic map of Bmb20, with genomic sequence undetermined in the area indicated. Shown below are three exon maps of possible Bmb20 forms that might contain extra unknown exons, with the unknown genomic region following exon 24 indicated as a ?.

For the PCR test with primers 1071 and 459 (designed to exon 135), only one band was detected in all life cycle stages (Figure 21). There was only amplification of one PCR product, of the expected size of 394 bp. The absence of additional PCR products suggests that there are no extra exons in between exon region 50-22-24 and exon 135.

The PCR with primers 1071 and 394 (designed to exon 93), showed inconclusive results, with three bands present in all life cycle stages, two of which match the predicted sizes 394 and 476. Figure 22, a photograph of the gel taken after 1.5 hours at 86 volts, shows three distinct bands: a band at approximately 370 bp (which probably corresponds with the predicted PCR product of 394 bp) and what appears to be a doublet at approximately 500 bp (presumably one of the bands corresponds to the predicted PCR product of 476 bp). This doublet could be the possible result of either an extra exon in the region, or the absence of one (or more) of the exons 50, 22, or 24. Because of the very small size difference between the two bands of the doublet (indistinguishable with any degree of accuracy or precision from this gel photograph), the gel was placed back in the electrophoretic apparatus and run for an additional hour at 86 V, in an attempt to get better resolution and separation of the possible doublet at 500 bp. Subsequent photographs showed the presence of only two bands, at 394 bp and approximately 500 bp, the sizes of predicted PCR products (data not shown). At this time, there is no good explanation or hypothesis with regard to the disappearing doublet.

A similar finding as that of the exon 93 PCR was encountered with the exon 174 PCR, done with primers 1071 and 343 (designed to exon 174). An initial examination of the gel after 1.5 hours run at approximately 86 volts indicated the presence of five possible bands (one at 370 bp, and then possible doublets at approximately 500 bp and 650 bp), three of which correspond to the predicted PCR products of sizes 394, 476, and 647 bp. The doublet at approximately 500 bp is consistent with the results of the exon 93 PCR (Figure 23). However, the resolution of this gel was poor, and when the gel continued to run for another hour at the same voltage, the presence of the doublets was gone and only three distinct bands were visible (data not shown). The initial examination of the exon 93 and exon 174 PCR products on a 2% agarose gel after one hour at 86 V, and the presence of multiple PCR products, more than were predicted, suggests the possibilities that either one or more of the exons in the 50-22-24 region may not be constitutively expressed, or that additional exons may be present in this region.

The results of this investigation regarding additional exons in the region of exons 50-22-24 is inconclusive. Additional work needs to be done to verify the presence or absence of additional exons in this region and whether or not these exons are constitutively expressed in *B. malayi*.

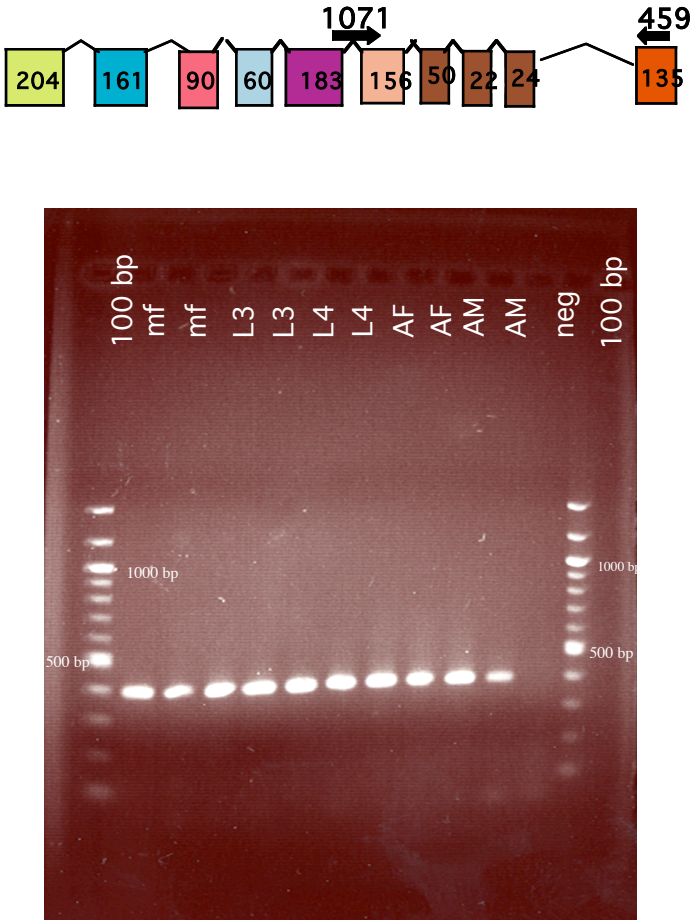

Figure 21. Photograph of PCR products, run on a 2% gel for 1 hour, 20 minutes at 86 V, from the PCR testing for the presence of extra exons in the 50-22-24 region of the gene. Forward primer 1071, spanning the exon boundary of constitutive exons 183 and 156, and reverse primer 459, designed to a sequence within exon 135, were used in the PCR on mf, L3, L4, AF and AM cDNA template. The expected size of the PCR product for this experiment was 394 bp, and a single band of about 400 bp is evident on this gel. The presence of only a single PCR product of the correct size thus suggests that there are no extra exons present in the region, spanning exon 24 and exon 135.

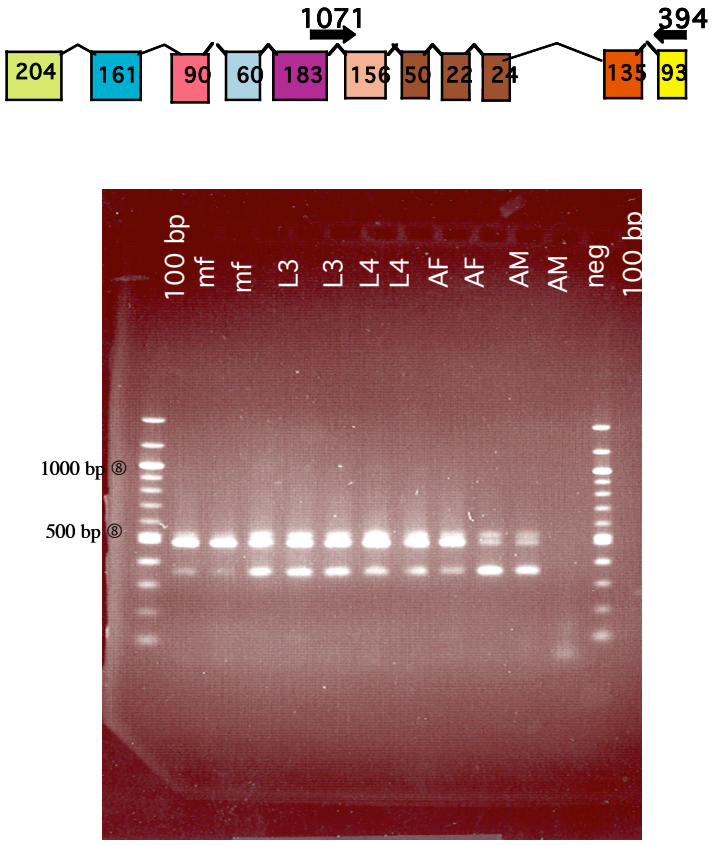

Figure 22. Photograph of PCR products, run on a 2% gel for 1 hour, 20 minutes, from a PCR testing for the presence of extra exons in the 50-22-24 region of the gene. Forward primer 1071, spanning the exon boundary of constitutive exons 183 and 156, and reverse primer 394, designed to a sequence within exon 93, were used in the PCR on mf, L3, L4, AF, and AM cDNA. The expected sizes of PCR product from this reaction were 376 and 476 bp in the absence of any additional exons. It appears as though there are three PCR products: a single band at approximately 400 bp, and a doublet at 500 bp in all stages. Because this is the second exon 'out' from the 50-22-24 region, in the absence of any extra exons, there should only be two PCR products. However, the presence of this doublet suggests one of two possibilities: either there is a very small extra exon present in the larger of the two 500 bp bands, or one or more of the exons 50, 22, and 24 may be absent from the PCR product that is the slightly smaller of the two bands at 500 bp.

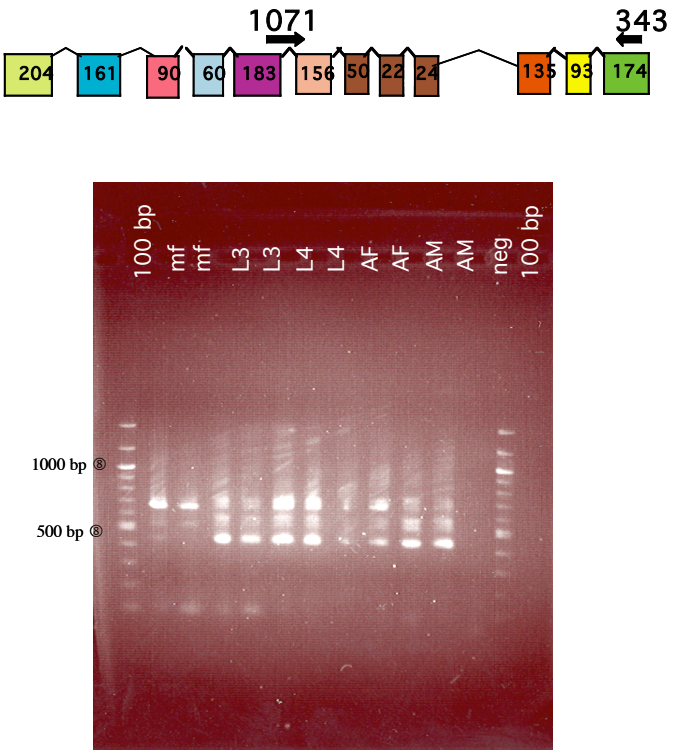

Figure 23. Photograph of PCR products, run on a 2% gel for 1 hour, 20 minutes, from a PCR testing for the presence of extra exons in the 50-22-24 region of the gene. Forward primer 1071, spanning the exon boundary of constitutive exons 183 and 156, and reverse primer 343 designed to a sequence within exon 174, were used in the PCR on mf, L3, L4, AF, and AM cDNA. It appears as though there are five PCR products visible: a single band at approximately 400 bp, a possible doublet at 500 bp, and a second possible doublet at approximately 650 bp, though the resolution of this gel was poor. The predicted sizes of PCR products, in the absence of any extra exons, were 394 bp, 476 bp, and 647 bp, consistent with three of the five bands present on the gel. Because this is the third exon 'out' from the 50-22-24 region, in the absence of any extra exons, there should only be three PCR products. However, the presence of these two possible doublets (one the same as found in the Exon 93 test, Figure 22) suggests one of two possibilities: either there is a very small extra exon present in the larger of the two 500 bp bands, or one or more of the exons 50, 22, and 24 may be absent from the PCR product that is the slightly smaller of the two bands in the doublets.

Part III. Quantitative RT-PCR

The splice variants b20-l and b20-n, due to their apparent upregulation in the L3 stage in the non-quantitative RT-PCs (Figures 17 and 18), were selected as candidates for further evaluation via quantitative RT-PCR. All life cycle stages, including L1 and L2, were tested using the quantitative RT-PCR method.

Inconclusive results for b20-n

Despite optimizing primer concentrations for use in a quantitative RT-PCR experiment testing for the presence of the b20-n splice variant, attempts to construct a relative standard curve for use in data analysis failed (data not shown). Purified PCR products from the PCR with primers designed to constitutive exons done on *B. malayi* L3 were used with the b20-n quantitative RT-PCR primers and probe in order to construct a standard curve. Poor amplification plots and very high Ct values suggested the possibility that the b20-n splice variant is not expressed at a high enough level to be detectable, and b20-n was no longer considered a good candidate for assessment using quantitative RT-PCR methods. A quantitative RT-PCR of b20-n in *B. malayi* was therefore not performed.

b20-l may be upregulated in L3 as compared to other life cycle stages

Ct values resulting from the PCR done with 10 ng template, but only on mf, L3, L4, AF and AM stages (due to lack of L1 and L2 parasite material) were analyzed using the standard curve method, with the mf stage designated as the calibrator (stage against which all other stages were compared). The highest level of expression of b20-l was found in the L3 stage, with approximately 53.5 times greater expression in the L3 than in the mf. When compared to the mf, the L4 had only 1.08 times the expression of b20-l, the AF expressed b20-l to a lesser extent than the mf, only 0.74 times as much, and the AM expressed 2.10 times the amount of b20-l as the mf stage (Figure 24). Therefore, the highest level of expression was found in the L3 stage, with the lowest level of expression of b20-l found in the AF. Though it was found in this experiment that the L3 had the highest level of expression of b20-l, the AM stage had the second highest level of expression of b20-l.

For the PCR done with 1 ng of template from all life cycle stages (L1, L2, L3, L4, AF and AM), inconclusive results were obtained. Because of the very small starting quantities of L1 and L2 parasite material, RNA yields were accordingly low, and the qRT-PCR could not be performed on 10 ng of template. For all life cycle stages except the L1 and L2, the level of expression of b20-l was undetectable. However, Ct values were obtained for both the target b20-l and endogenous control NDK in the L1 and L2 stages.

Because a difference of approximately 3.3 Ct values can be estimated per log-fold dilution of template if assuming a reaction efficiency of 100%, Ct values were *predicted* for 10 ng of L1 and L2 template using the data obtained from the 1 ng of template used in this experiment. In this way, an interpretive (or extrapolated) comparison of the results obtained from the data using 1 ng of L1 and L2 cDNA template could be done with the results obtained from the data resulting from 10 ng of mf, L3, L4, AF, or AM cDNA template. Specifically, these predicted Ct values for both b20-l and NDK expression in L1 and L2 were determined by subtracting 3.3 from the Ct values obtained at 1 ng to estimate what the Ct values for the L1 and L2 might have been had 10 ng of template been used. While these results are therefore just predictions, they do suggest potential patterns of expression of b20-l in the L1 and L2 stages. The result of this investigation (these predicted 10 ng values for the L1 and L2) suggests that b20-l is greatly upregulated in the L2 stage, with approximately 53326 times greater expression than in the mf (the mf was again chosen as the calibrator). There appeared to be some level of expression in the L1 stage, with about 41963 times greater expression in that stage as compared to the mf. When compared with the values obtained with 10 ng of mf, L3, L4, AF and AM template, the stage with the second highest level of expression of b20-l after the L2 was the L3 (53.5 times greater than the mf), followed by the L1 and then the AM (Figure 25). However, these are only predicted, potential

results based on the extrapolation of data from the L1 and L2 reactions done on 1 ng of template.

The results of this quantitative RT-PCR therefore suggest that b20-l is upregulated in the L3 stage as compared to the mf, L4, AF and AM stages. However, the expression pattern of b20-l is still unknown in the early larval stages L1 and L2. It is possible that b20-l is also upregulated in these larval stages, though that is only a prediction based on extrapolated data at this point. It should be noted that neither of these results, based on only one qRT-PCR experiment, are statistically significant.

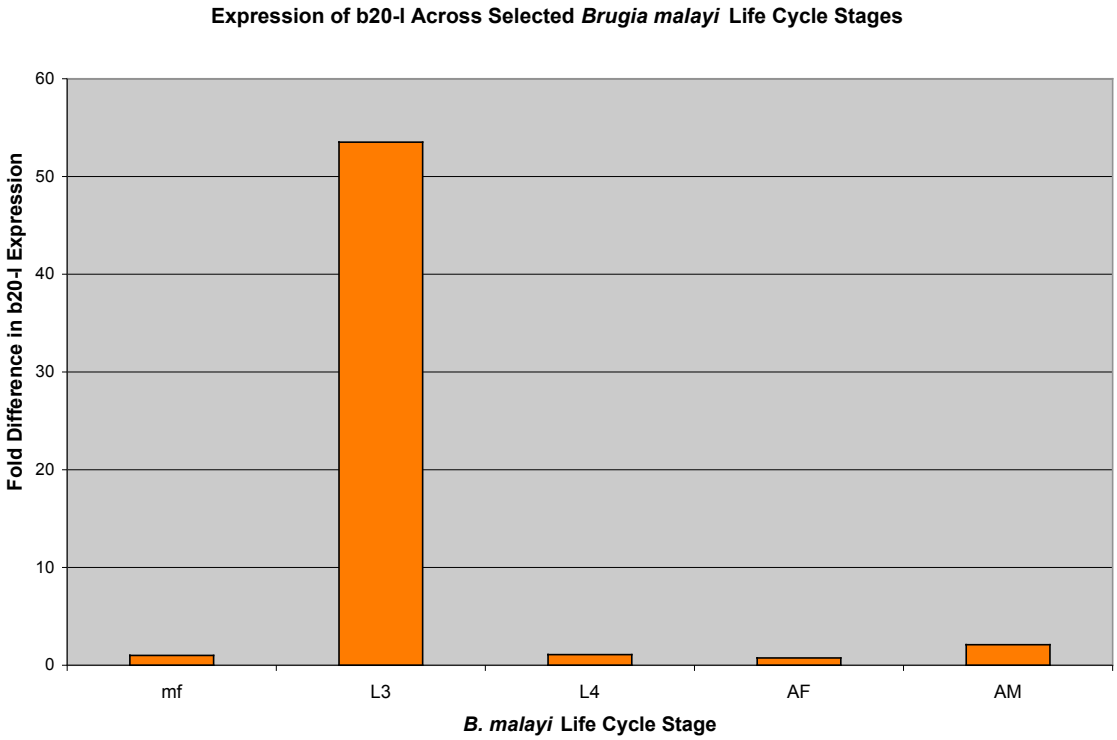

Figure 24. Graph showing the differential expression of b20-l across the *B. malayi* life cycle stage as determined by qRT-PCR methods. Evident is the upregulation of b20-l in the L3 stage as compared to all other stages. b20-l was found to be expressed 53.5 times more in the L3 than the mf stage, as compared to the L4, which was 1.08 times greater; the AF, which was only 0.74 times greater, and the AM, expressed 2.10 times the amount found in mf. This data confirms the predicted upregulation of b20-l in L3 as indicated by the non-quantitative RT-PCR and subsequent signal detection with gel electrophoresis.

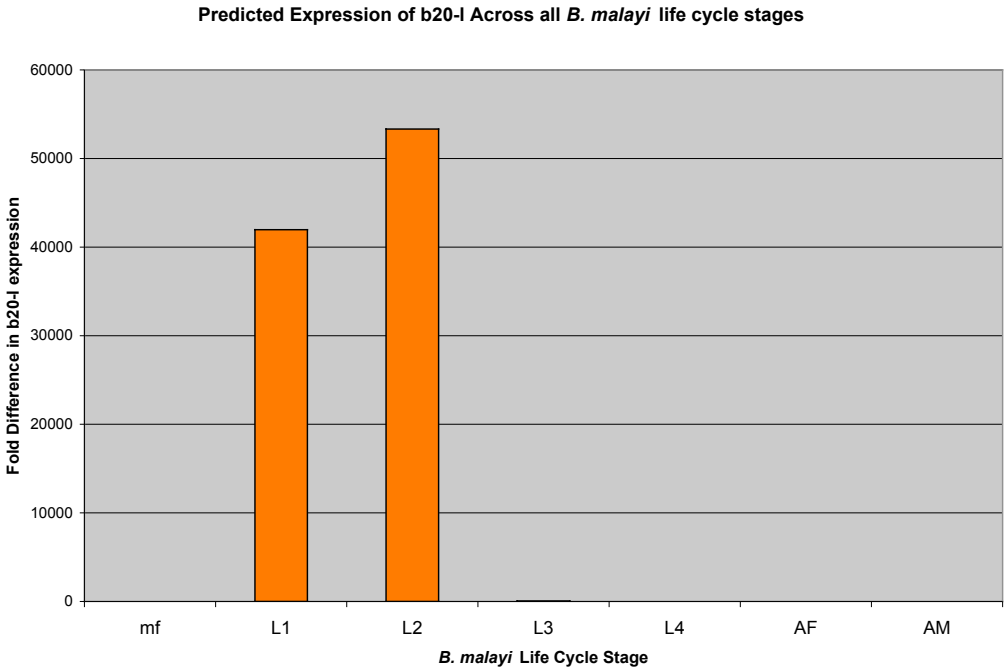

Figure 25. Graph showing the differential expression of b20-l across the *B. malayi* life cycle stage as determined by qRT-PCR methods, using extrapolated L1 and L2 1 ng of template data. Evident is the upregulation of b20-l in the L2 and L1 stages as compared to all other stages. b20-l was found to be expressed 41963 times more in the L1 and 53326 times more in the L2 than in the mf stage, as compared to the L3, which had 53.5 times greater expression than the mf stage. The L1 and L2 express 784 times and 996.75 times b20-l, respectively, than the L3. This data is based on predicted and extrapolated values due to the lack of parasite material. While the relatively high levels of amplification might also indicate a problematic qRT-PCR reaction, further work is necessary to determine the level of expression of b20-l in L1 and L2 (as well as the rest of the life cycle).

DISCUSSION

RNA Extraction

The RNA yield from the parasites was lower than expected. In addition to the microscopic size of *B. malayi* specimens, as well as the relatively low numbers of worms in some cases, incomplete interruption of the worm cuticle may be partially responsible for the low yields of extracted RNA from the number of parasites used (Table 4).

RT-PCR: Evaluation of Splice Variant Expression

Overall b20 Splice Variant Expression

The variety of b20 splice variants expressed in all of the life cycle stages of *B. malayi* has been illustrated by this work. Although the function of b20 remains unclear at this point, clearly the parasite is utilizing much energy and resources on expressing a multitude of forms across all developmental stages. This evidence, combined with RNAi studies done on the b20 ortholog in *C. elegans*, gei-16, supports a developmental role for this gene (Fraser *et al*., 2000). Additional evidence of a developmental role for this gene includes studies in *C. elegans* showing that gei-16 interacts with GEX-3, an essential factor of tissue morphogenesis (Tsuboi *et al.*, 2002). Recently, gei-16 has also been identified as a candidate for interaction with LIN-5, required for spindle positioning and chromosome segregation (Fisk Green *et al*., 2004).
Evaluation of specific splice variant expression patterns in *B. malayi* may help

elucidate which splice variants are crucial for which stages or aspects of worm development.

The primary purpose of this experiment was to identify the expression pattern of b20 splice variants in *B. malayi*, with the additional goal of identifying any L3 specific splice variants as potential diagnostic assay candidates. Previous plaque screenings of the *B. malayi* L3 cDNA library had identified the splice variants b20-j, b20-l, b20-a and b20-e in the L3 stage and at least eight additional b20 splice variant forms were identified in various stages of *Onchocerca* (Walls, 2001; Laney 2002). The information regarding exon arrangements and the constitutive versus alternative expression of exons obtained from these plaque screen studies allowed the design of primers to do RT-PCR analysis of b20 expression patterns in this study. RT-PCR has been shown to be a sensitive method capable of detecting low levels of gene expression in *B. malayi* (Li *et al*., 2004) and the results of this study demonstrated the detection of many more splice variants in the L3 stage of *B. malayi* than the four previously identified by plaque screenings. However, the exact exon structure of these splice variants has not yet been characterized.

A large number of b20 splice variants were identified as being expressed across the *B. malayi* life cycle using RT-PCR methods (Tables 5 and 6). The RT-PCR results using primers designed to constitutive exons showed that many different splice variants were being expressed in all of the life cycle stages of *B. malayi*, while the presence of at least two bands restricted to the

L3 stage suggest the existence of two L3-specfic splice variants (Figure 11). Those putative L3-specific PCR products were represented on the agarose gel as bands relatively less intense than other PCR products present in both the L3 and other stages. This might suggest the decreased expression of those L3-specific splice variants with respect to the expression of other splice variants, either in L3 or throughout the lifecycle. This would decrease their prospects as good diagnostic candidates for an L3-specific assay due to decreased sensitivity. However, because many splice variants were being amplified in that one PCR, the issue of competition could be a factor resulting in the apparent decreased expression of the L3-specific PCR products.

Though it appears that L3-specific splice variants may exist, it was not possible to separate and isolate those putative L3-specific PCR products from the gel because the sizes were too similar to many of the other PCR products present. Therefore, the gel extraction and sequencing of only the L3-specific PCR products was not possible at this time. Without the sequence data, the identification and verification of those potential L3-specific splice variants remains unknown.

Although some PCR products appear to be restricted to specific life cycle stages, the majority of splice variants seem to be expressed in all stages (Figure 11, Table 6). However, this cannot be definitively ascertained by this constitutive PCR method because many of the splice variants would result in products of a similar size. Thus PCR designed to amplify specific splice

variants is necessary to evaluate the stages of expression of any particular form.

Splice Variant Specific RT-PCR

Splice variant-specific PCR tests, in addition to the constitutive exon PCR, clearly indicate that there are several different b20 forms of mRNA in *B. malayi*. However it should be clarified that all of these PCRs were done using primers designed to the form-specific *regions*. Therefore, please note that the absolute presence of the entire splice variant as depicted in Figure 6 has not actually been determined; only the form-specific *region* of that variant was tested for. It remains possible that other splice variant forms might also contain the respective form-specific region, but may vary with regard to either the upstream or downstream regions of the forms. For example, while the results of the non-quantitative RT-PCRs might be extrapolated to suggest that b20-n may be upregulated in the L3 stage as compared to the other life cycle stages (Figure 18), the results of the RT-PCR only suggest that the *form-specific region* of b20-n is upregulated in the L3 stage relative to other life cycle stages. There may be multiple forms that include the exact same region, but whose splicing patterns and expression patterns are different in either upstream or downstream regions (or both). With regard to the search for an upregulated or L3-specific diagnostic assay candidate, only the *region* would be required to be specific or upregulated. While the term splice variant has

been used for simplicity and convenience in this work, it must be noted that in most cases, these data only support the presence or absence of a specific splice variant *region*.

In addition to the constitutive RT-PCR, five specific splice variants were tested for and identified as being expressed across the life cycle of *B. malayi* (b20-i, j, k, l, n). These splice variants correspond to those previously characterized in *O. volvulus*, though by those plaque screenings, most splice variants were found to be stage restricted. In addition, this study also identified the presence of two possible new splice variants, designated b20-q and b20-r, that had not previously been identified in either species. Primers designed to amplify these predicted splice variant forms resulted in PCR products of the expected size. However, without sequencing those PCR products (predicted to be b20-q and b20-r), it is impossible to know the exact exon arrangement of the splice variants that were amplified. Nevertheless, the fact that a PCR product of the appropriate size resulted from amplification with primers that span specific exon junctions is positive evidence that these new splice variant forms exist.

Quantitative RT-PCR

Initially, two splice variant forms (b20-l and b20-n) were selected for evaluation by quantitative real-time RT-PCR. However, the qRT-PCR testing for the b20-n splice variant resulted in undetectable Ct values, suggesting

levels of expression of b20-n that were too low for accurate analysis by qRT-PCR. Since the expression profile of b20-n could not be established, it is clearly not a good candidate for a diagnostic assay at this time.

The results of the b20-l qRT-PCR experiment done with 10 ng of cDNA template suggest that b20-l is highly upregulated in L3 with respect to the other life cycle stages, excepting L1 and L2 stages (Figures 24 and 25), situating it as a possible candidate for an L3-specific diagnostic target. However, the predicted expression of b20-l in the L1 and L2 stages, based on data extrapolated from the experiment performed with only 1 ng of L1 and L2 template, suggests that b20-l is also upregulated in both the L1 and L2 stages. It may even be upregulated to a much greater extent in the L2 than the L3 (Figure 25). While it must be remembered that these data from the L1/L2 stages are based on extrapolation, and therefore cannot strictly be compared to the L3 data (resulting from a different experiment with 10 ng of template), it does suggest that further investigation into the expression pattern of b20-l in both the L1 and L2 is necessary if b20-l were to be seriously considered as a candidate target for an L3-diagnostic assay. However, the total expression level of b20-l even in the L3 stage is relatively low, and the relatively low yields of RNA from these parasites point to the importance of using a gene transcript that is expressed at a relatively high level as a diagnostic candidate in an RT-PCR assay.

Despite the complications presented by the L1 and L2 data, interesting observations can still be obtained from the qRT-PCR experiment performed on 10 ng of mf, L3, L4, AF, and AM cDNA. While b20-l was found to be most highly expressed in L3 (at approximately 53 fold more than the mf stage), the stage with the next highest level of expression, at 2 fold more than the mf stage, was adult male, and the lowest level of expression was found in the female (Figure 24). Interestingly, Taylor (1995) found with *in situ* hybridization that transcription of Ovb20 is confined only to larval stages, with initiation in embryos and maximum production during development from L2 to L4. The low level of B20 protein found in adult females was hypothesized to be present due to the developing mf in utero (Taylor, 1995). Though those experiments were done in *O. volvulus* and not *B. malayi*, the results are contradictory to what was found using RT-PCR methods in this study. While the highest levels of expression of Bmb20-l were detected in L3, after that, greater levels of expression of Bmb20-l were detected in the adult male stage than in the other stages (mf, L4, and AF).

Importance of b20

The results of this study, both quantitative and non-quantitative, contribute to a better expression profile of the b20 gene in *B. malayi*. Despite the possibility that the most promising candidate, b20-l, may be upregulated to an even greater extent in the L2 as in the L3 (precisely the worse case scenario

for an L3-specific diagnostic assay), the overall low levels of expression of b20 also indicate its insufficiency as a reliable target in a diagnostic assay. A highly-upregulated L3-specific gene is the ideal, because of the necessity for a specific as well as sensitive assay. While no L3-specific splice variants have yet been identified, the possibility of any b20 splice variants being appropriate targets for use in a diagnostic assay has been mostly ruled out. This is crucial information to have prior to continuing further tests due to the scarcity of parasite material available, and energies can now be focused on searching for other suitable candidates.

Though b20-l may not be suitable as a target for use in a diagnostic assay, its definitive upregulation in the L3 stage may still make it an appropriate target for a drug as the L3 stage is the human infective stage. If the function of b20 is in fact developmental as suggested by *C.elegans* work, perhaps an upregulation of b20-l may be due to the requirement of that protein for the molt or development to the L4 stage. If the L3 to L4 molt can be halted in the human host, the establishment of the parasite infection would be terminated. The function of b20 as yet remains unknown, but the fact that there are a number of splice variants (all of those identified by the PCR designed to constitutive exons) only strengthens the hypothesis that this must be a gene of some importance; *B. malayi* is expending quite a bit of energy to make all these splice variants. If these splice variants are particularly important in the L3 stage, as suggested by upregulation (at least in the case of

b20-l), then because L3 is the human infective stage, they may be suitable targets for new drugs specific for the L3 stage. There appears to be some stage regulation concerning many of the Bmb20 splice variants identified in this study. It is possible that there are differences in immunogenicity, and thus perhaps in the human immune response to these varying splice variants, as each encodes a different protein. The localization of B20 protein to the hypodermis and cuticle of L3 (in *O. volvulus*, and presumably similar in *B. malayi*) suggests B20 is secreted; at the very least, it is present on the exterior of the worm and thus accessible to the host immune system (Taylor, 1995). Future functional investigations employing the technique of RNAi in *B. malayi* will help further elucidate the function of b20.

Further Questions and Future Work

This was only a preliminary study concerning the expression profile of b20 splice variants in *B. malayi*. Certainly, future work will continue to examine the expression profile of this complex gene with its many splice variants. Immediate experiments to be completed include continued qRT-PCR experiments, ideally with adequate amounts of L1 and L2 template. Repeated experiments to verify the results of the one qRT-PCR performed in this study are also necessary to examine biological significance.

Other avenues for future work on Bmb20 include the sequencing of the PCR products predicted to be the ‘new’ splice variants b20-q and b20-r.

Additionally, there remain many unanswered questions due to the fact that all of these experiments were only testing for form specific *regions* of Bmb20 splice variants. While the results of this study have contributed to a greater understanding of the expression profile of b20 in *B. malayi*, splicing patterns in other regions of the gene remain unknown, such as the upstream region containing exon 91. While it is now known that exon 91 is not expressed in a stage specific manner, the particular splicing patterns of this exon (and for that matter, most exons in the upstream region of Bmb20) are not known. cDNA library screenings are ongoing in the Williams laboratory to isolate complete clones and to sequence and identify additional exon arrangements in an attempt to fully understand the variety of b20 splice variants that are being expressed in this parasite. Though it is true that for the purposes of identifying an L3-specific target, the specificity of a particular region is more important than the presence of a specific splice variant form, it would be useful to know the expression pattern of all b20 splice variants in *B. malayi*.

This study has therefore shown that RT-PCR and qRT-PCR methods can be valuable in the detection of expressed genes, particularly genes with low levels of expression. Five specific b20 splice variants have been identified across the life cycle in *B. malayi*, and many more splice variant forms have been identified but not yet characterized. The differential expression of one splice variant, b20-l, has been examined using qRT-PCR methods and shown to be upregulated in the L3 stage, at least with respect to all stages except L1

and L2. While no Bmb20 splice variants have been found to be appropriate potential candidates for the target of the L3-specific assay, the presumed developmental role of b20 in the human infective stage warrants continued investigation into this gene as a possible drug target.

APPENDIX

Appendix A: cDNA synthesis

cDNA synthesis Reaction Mix From Applied Biosystems TaqMan Gold RT-PCR Protocol

Reaction done in a total volume of 100 μl.

	μl
RNAse-free water (DEPC water)	28.5
10 X TaqMan RT Buffer	10.0
25 mM MgCl2 (5.5 mM)	22.0
dNTPs (500 μM each)	20.0
Oligo (dT) (2.5 mM)	5.0
RNase Inhibitor (0.4 U/μl)	2.0
Multiscribe Reverse Transcriptase (1.25 U/μl)	2.5
RNA template (1 μg)	10.0

Appendix B: RT-PCR

RT-PCR Reaction Mix From Applied Biosystems TaqMan Gold RT-PCR Protocol

Reaction done in a total volume of 50 μl.

	μl
RNase-free water	22.75
10X TaqMan PCR Buffer	5.0
25 mM MgCl2	11.0
dNTPs	4.0
Forward Primer	1.0
Reverse Primer	1.0
TaqGold DNA Polymerase	0.25
cDNA template	5.0

Appendix C: Q RT PCR

Q-RT-PCR Reaction Mix. Adapted from Ben-Wen Li and Amy C. Rush at Washington University (Saint Louis, MO).

Reaction done in a total volume of 25 μl.

	μl
ABI RT-PCR Universal Master Mix	7.9
Specific ABI TaqMan VIC/TAMRA probe (250 nM)	6.25
Specific forward primer (volume varied; 50 nM to 900 nM)	
Specific reverse primer (volume varied; 300 nM to 900 nM)	
RNase-free water (DEPC water) (volume varied)	
10 ng cDNA template	1.0

LITERATURE CITED

Abdel-Wahab N, Kuo YM, Wu Y, Tuan RS, Bianco AE (1996). OvB20, an *Onchocerca volvulus*-cloned antigen selected by differential immunoscreening with vaccination serum in a cattle model of onchocerciasis. *Mol. Biochem. Parasitol*. 76, 187-199.

Aboobaker AA and Blaxter ML (2003). Use of RNA interference to investigate gene function in the human filarial nematode parasite *Brugia malayi*. *Mol. Biochem. Parasitol*. 129, 41-51.

Bain O and Babayan S (2003). Behaviour of filariae: morphological and anatomical signatures of their life style within the arthropod and vertebrate hosts. *Filaria Journal* 2(16). Available at: www.filariajournal.com/content/2/1/16.

Baird JB, Louis Charles J, Streit TG, Roberts JM, Addiss DG, Lammie PJ (2002). Reactivity to bacterial, fungal, and parasite antigens in patients with lymphedema and elephantiasis. *Am. J. Trop. Med. Hyg.* 66, 163-169.

Bandi C, Anderson TJC, Genchi C, Blaxter ML (1998). Phylogeny of *Wolbachia* in filarial nematodes. *Proc. R. Soc. Lond., Series B-Biological Sciences* 265, 1-7.

Blaxter ML, Raghavan N, Ghosh I, Guiliano D, Lu W, Williams SA, Slatko B, Scott AL (1996). Genes expressed in *B. malayi* infective third stage larvae. *Mol. Biochem. Parasitol*. 77, 77-96.

Blaxter ML, De Ley P, Garey J,. Liu LX, Scheldeman P, Vierstraete A, Vanfleteren J, Mackey LY, Dorris M, Frisse LM, Vida JT, Thomas WK (1998). A molecular evolutionary framework for the phylum Nematoda. *Nature* 392, 71-75.

Blaxter M, Aslett M, Guiliano D, Daub J, and the FGP (1999). Parasitic helminth genomics. *Parasitology* 118, S39-S51.

Blumenthal T and Steward K (1997). RNA Processing and Gene Structure. In *C. elegans* II in Cold Spring Harbor Laboratory Press. Edited by D. Riddle, T. Blumenthal, B. Meyer, and J. Priess. Cold Spring Harbor Press.

Bockarie MJ, Fishcer P, Williams SA, Zimmerman PA, Griffin L, Alpers MP, Kazura JW (2000). Application of a polymerase chain reaction-ELISA to detect *Wucheria bancrofti* in pools of wild-caught *Anopheles* punctulatus in a filaraisis control area in Papua New Guinea. *Am. J. Trop. Med. Hyg.* 62, 363-367.

Brudno M, Gelfand MS, Spengler S, Zorn M, Dubchak I, Conboy JG (2001). Computational analysis of candidate intron regulatory elements for tissue-specific alternative pre-mRNA splicing. *Nucleic Acids Res* 29, 2338-2348.

Burglin T, Lobos E, Blaxter ML (1998). *C. elegans* as a model for parasitic nematodes. *Int J Parasitol* 28, 395-411.

C. elegans Sequencing Consortium (1998). Genome sequence of the nematode *C. elegans*: a platform for investigating biology. *Science* 2011: 2012-2018.

Cox FEG (2000) Elimination of lymphatic filariasis as a public health problem. *Parasitol Today* 16, 135.

deAlmeida AB, eSilva MCM, Braga C, Freedman DO (1998). Differences in the frequency of cytokine-priducing cells in antigenemic and nonantigenemic individuals with Bancroftian filariasis. *Infect Immun*. 66, 1377-1383.

Despommier D (1995). *Onchocerciasis* in Parasites in Human Tissues, Edited by Thomas C. Orihel, Lawrence R. Ash. ASCP Press.

Dreyer G, Noroes J, Figueredo-Silva J, Piessens WF (2000). Pathogenesis of lymphatic disease in bancroftian filariasis: a clinical perspective. *Parasitol Today*. 16, 544-548.

Eberhard ML, Hightower AW, Addis DG, Lammie PJ (1997). Clearance of *Wucheria bancrofti* antigen after treatment with diethylcarbamazine or ivermectin. *Am. J. Trop. Hyg*. 57, 483-486.

Evans DB, Gelband H, Vlassof C (1993) Social and economic factors and the control of lymphatic filariasis: a review. *Acta Tropica* 53, 1-26.

Fischer P, Liu X, Lizotte-Waniewski M, Kamal IH, Ramzy RM, Williams SA (1999). Development of a quantitative, competitive PCR-ELISA for the detection of *W. bancrofti* DNA. *Parasitol Res*, 85, 176-83.

Fisk Green R, Lorson M, Walhout AJM, Vidal M, van den Heuvel S (2004). Identification of critical domains and putative partners for the *Caenorhabditis elegans* spindle component LIN-5. *Mol Gen Genomics* 271, 532-544.

Foster J, Ganatra M, Kamal I, Ware J, Makarova K, Ivanova N, Bhattacharyya A, Kapatral V, Kumar S, Posfai J, Vincze T, Ingram J, Moran L, Lapidus A, Omelchenko M, Kyrpides N, Ghedin E, Wang S, Goltsman E, Joukov V, Ostrovskaya O, Tsukerman K, Mazur M, Comb D, Koonin E, Slatko B (2005). The *Wolbachia* genome of *Brugia malayi*: endosymbiont evolution within a human pathogenic nematode. *PLoS Biol* 3, e121

Foster JM and Johnston DA (2002). Helminth genomics: from gene discovery to genome sequencing. *TRENDS in Parasitology* 18, 241-2.

Fraser AG, Kamath RS, Zipperlen P, Martinez-Campos M, Sohrmann M, Ahringer JA (2000). Functional genomic analysis of *C. elegans* chromosome I by systematic RNA interference. Nature 408, 325-330.

Freedman DO (1998). Immune Dynamics in the Pathogenesis of Human Lymphatic Filariasis. *Parasitol Today* 14, 229-234.

Ghedin E, Wang S, Foster JM, Slatko B (2004). First sequenced genome of a parasitic nematode. *TRENDS in Parasitology*, 20, 151-53.

Goodman DS, Orelus JN, Roberts JM, Lammie PJ, Streit TG (2003). PCR and mosquito dissection as tools to monitor filarial infection levels following mass treatment. *Filaria Journal* 2(11). Available at: www.filariajournal.com/content/2/1/11.

Gravely BR (2001). Alternative splicing: increasing diversity in the proteomic world. *TRENDS in Genetics* 17, 100-107.

Gregory WF, Atmadja AK, Allen JE, Maizels RM (2000). The abundant larval trnascript-1 and –2 genes of *Brugia malayi* enocode stage-specific candidate vaccine antigens or filariasis. *Infect Immun*. 68, 41479 – 41749.

Guevara AG, Viera JC, Lilley BG, Lopez A, Viera N, Rumbea J, Collins R, Katholi CR, Unnasch TR (2003). Entomological evaluation by pool screen polymerase chain reaction of *Onchocerca volvulus* transmission in Ecuador following mass Mectizan distribution. *Am. J. Trop. Med. Hyg*. 68, 222-227.

Guiliano DB, Hall N, Jones SJM, Clark LN, Corton CH, Barrell BG, Blaxter ML (2002). Conservation of long-range synteny and microsynteny between the genomes of two distantly related nematodes. *Genome Biology* 3(10). Available at: http://genomebiology.com/2002/3/10/research/0057.1

Huang X, Duran E, Diaz F, Xiao H, Messer WS Jr, Komuniecki R (1999). Alternative-splicing of serotonin receptor isoforms in the pharynx and muscle of the parasitic nematode, *Ascaris suum*. *Mol. Biochem. Parasitol*., 101, 95-106.

Hussain R, Hamilton RG, Kumaraswami V, Adkinson NF, Ottesen EA (1981). IgE response in human filariasis. I Quantitation of filarial-specific IgE. *J. Immunol*. 127, 1623 – 1629.

Jin J, Poole CB, Slatko BE, McReynolds LA (1999). Alternative splicing creates sex-specific transcripts and truncated forms of the furin protease in the parasite *Dirofilaria immitis*. *Gene* 237, 161-175.

Keiser PB and Nutman TB (2002) Update on lymphatic filariasis. *Curr Infect Dis Reps* 4, 65-69.

Kumaraswami V (2000). *The Clinical Manifestations of Lymphatic Filariasis* in Lymphatic Filariasis, Edited by Thomas Nutman, Imperial College Press.

Laney, SJ (2002). Genomic organization of four vaccine candidate genes in *Onchocerca volvulus* and the complex alternative splicing of b20-1. Thesis (MA), Smith College, Northampton, MA, 117 pages.

Li, B, Rush AC, Tan J, Weil GJ (2004). Quantitative analysis of gender-regulated transcripts in the filarial nematode Brugia malayi by real-time RT-PCR. *Mol. Biochem. Parasitol*. 137, 329-337.

Martin KJ and Pardee AB (2000). Identifying expressed genes. *PNAS* 97, 3789-3791.

Michael E, Grenfell BT, Bundy DAP (1994). The Association between Microfilaremia and Disease in Lymphatic Filariasis. *Proc. R. Soc. Lond., Series B- Biological Sciences* 256(1345), 33-40.

Molyneux DH, Davies JB (1997). Onchocerciasis control : Moving towards the millennium. *Parasitol Today* 13, 418-425.

Molyneux DH, Zagaria N (2002) Lymphatic filariasis elimination: progress in global programme development. *Ann Trop Med Parasitol.* 96, S15-S40.

O'Neill SL, Giordano R, Colbert AME, Karr TL, Robertson HM (1992). 16S rRNA phylogenetic analysis of the bacterial endosymbionts associated with cytoplasmic incompatibility in insects. *Proc. Natn. Acad. Sci. USA*. 89, 2699-2702.

Ottesen EA, Skvvaril F, Tripathy SP, Poindexter RW, Hussein R (1985). IgG subclasses in human filariasis: prominence of IgG4 in the IgG antibody response to human filariasis. *J. Immunol*. 134, 2702 – 2712.

Ottesen EA (2000) Editorial: the global programme to eliminate lymphatic filariasis. *Trop Med Int Health* 5, 591-594.

Ramzy RM, Farid HA, Kamal IH, Ibrahim GH, Morsy ZS, Faris R, Weil GJ, Williams SA, Gad AM (1997). A PCR-based assay for the detection of *W. bancrofti* in human blood and *Culex pipiens. Trans R Soc Trop Med Hyg* 91, 156-60.

Saunders, LJ (2000). The localization, differential expression, and potential immunological role of thioredoxin peroxidase-2 (TPX-2) in the filarial parasite *Brugia malayi*. Thesis (PhD), University of Massachusetts, Amherst, MA, 156 pages.

Scott AL (2000) *Lymphatic-dwelling Filariae* in Lymphatic Filariasis, Edited by Thomas Nutman, Imperial College Press.

Stepek G, Houston KM, Goodridge HS, Devaney E, Harnett W (2004). Stage-specific and species-specific differences in the production of the mRNA and protein for the filarial nematode secreted product, ES-62. *Parasitology* 128, 91-98.

Taylor MJ, Abdel-Wahab N, Wu Y, Jenkins RE, Bianco AE (1995). *Onchocerca volvulus* larval antigen, OVB20, induces partial protection in a rodent model of Onchocerciasis. *Infection and Immunity* 63, 4417-4422.

Taylor, M (2002). A new insight in the pathogenesis of filarial disease. *Curr Mol Med*. 2, 299-302.

Townson S, Hutton D, Siemienska J, Hollick L, Scanlon T, Tagboto SK, Taylor MJ (2000). Antibiotics and *Wolbachia* in filarial nematodes: antifilarial activity of rifampicin, oxytetracycline and chloramphenicol against *Onchocerca gutturosa*, *Onchocerca lienalis* and *Brugia pahangi*. *Ann Trop Med Parasitol*. 94, 801-16.

Tsuboi D, Qadota H, Kasuya K, Amano M, Kaibuchi K (2002). Isolation of the interacting molecules with GEX-3 by a novel functional screening. *Biochemical and Biophysical Research Communications* 292, 697-701.

Walls, CD (2001). Alternative splicing of the b20 gene in two filarial species. Thesis (Honors) Smith College, Northampton MA, 135 pages.

Weil GJ, Sethumadhavan KV, Santhanam S, Jain DC, Ghosh DK (1998). Persistence of parasite antigenemia following diethylcarbamazine therapy of bancroftian filariasis. *Am. J. Trop. Med. Hyg*. 38, 589-595.

Williams SA and the FGP, Johnston DA and the SGP (1999). Helminth genome analysis: the current status of the filarial and schistosome genome projects. *Parasitology*, 118, S19-S38.

Williams SA, Laney SJ, Biewert L, Saunders LJ, Boakye DA, Fischer P, Goodman DS, Helmy H, Hoti SL, Lammie PJ, Pilchart C, Ramzy R, Ottesen EA (2002a). The mosquito PCR project: to develop a rapid assessment tool for the detection of *W. bancrofti* infected mosquitoes. *Ann Trop Med Parasitol* 92(Supplement 2), 541-46.

Williams SA, Laney SJ, Bierwert LA, Saunders LJ, Boakye DA, Fischer P, Goodman D, Helmy H, Hott SL, Vasuki V, Lammie PJ, Plichart C, Ramzy RM, Ottesen EA (2002b). Development and standardization of a rapid, PCR-based method for the detection of *Wucheria bancrofti* in mosquitoes, for xenomonitoring the human prevalence of bancroftian filariasis. *Annals of Tropical Medicine and Parasitology*. 96, S41-S46.

World Health Organization (2000) Malaria. *Weekly Epidemiological Record* 29, 233-240.

World Health Organization (2001) Lymphatic filariasis. *Weekly Epidemiological Record* 20, 149-156. Available at: http://www.filariasis.org

Xie, H, Bain O, Williams SA (1994). Molecular phylogenetic studies on filarial parasites based on 5S ribosomal spacer sequences. *Parasite* 1, 141-151.

Yameogo L, Toe L, Hougard JM, Boatin BA, Unnasch TR (1999). Pool screen polymerase chain reaction for estimating the prevalence of *Onchocerca volvulus* infection in *Simulium damnosum sensu lato*: results of a field trial in an area subject to successful vector control. *Am. J. Trop. Med. Hyg*. 60, 124-128.